Filamentary Tracks Formed in Transparent Optical Glass by Laser Beam Self-Focusing. II. Theoretical Analysis*

Edwin L. Kerr

Perkin-Elmer Corporation, 50 Danbury Road, Wilton, Connecticut 06897

(Received 14 January 1971)

An electrostriction mechanism for laser-beam self-focusing and track formation in transparent optical glass is analyzed theoretically. Electrostrictive self-focusing occurs when a laser pulse of sufficiently high power and rapid rise time passes through a transparent medium. For a pulse duration of 50 nsec, trapping thresholds vary from 20 kW to 2 MW. During self-focusing, the beam collapses to a small radius. In solid dielectrics, self-focusing causes permanent damage in the form of isolated regions of gross fracture, termed "damage stars" and long straight tracks of very fine fractures. Typical tracks have a diameter of a few wavelengths of light and extend up to several centimeters. Self-focusing occurs because of an interaction between light and sound. The laser beam electrostrictively excites an ultrasonic cylindrical disturbance or sound wave. The sound wave initially increases the refractive index along the beam axis. This focuses the beam into a waveguide channel called a filament. In the filament, the intensity is so high that many nonlinear mechanisms may occur, leading to damage and track formation. This paper analyzes only the self-focusing mechanism, not the various damage mechanisms. We assume the beam always remains Gaussian. The propagation of the beam is described by the quasioptics beam-tracing equation, which includes the effects of diffraction. The sound wave and beam-tracing equations are solved in several approximate models. A trapping threshold is derived for three pulse shapes, covering the steady-state, transitional, and transient regimes of pulse duration and beam size. There is a trapping-power coefficient K for each material, calculable from the density, speed of sound for a compression wave or elastic moduli, and refractive index at the laser wavelength. A formula for computing the power to achieve a given constant maximum intensity I as a function of beam size, and pulse duration, and trapping-power coefficient is derived. Values of this given constant intensity have been selected so the constant-intensity curve closely matches experimental track-formation thresholds for three optical glasses. The results are $K = 221$ kW and $I = 2.5$ GW/cm^2 for dense flint glass, $K = 937$ kW and $I = 60$ GW/cm^2 for borosilicate crown glass, and $K = 1119$ kW and $I = 180$ GW/cm^2 for fused silica, at a fixed pulse duration of 55 nsec and a laser wavelength of 694.3 nm. A computer movie of beam trapping shows the collapse of the beam to a relatively constant small radius, which causes track formation. It also shows the extremely rapid upstream motion of the focal points at speeds greater than 100 times the speed of sound. The long period of time they dwell at the upstream end of their motion explains the appearance of damage stars at the upstream ends of the tracks.

I. INTRODUCTION

Since 1964, a large number of papers have reported laser damage to transparent solid dielectrics.[1-57] In this paper, our attention is limited to track formation, i.e., the formation of a damage feature collinear with the incident laser beam, many times longer than its diameter. Papers describing track formation explicitly have been classified separately in Table III.[1-20] The phenomenon is evidently related to laser-beam trapping in liquids.[58-98] A number of authors have analyzed the conditions under which a laser beam may focus itself into a long thin filament and propagate without diffraction spreading.[99-130] In liquids, the Kerr effect is the predominant self-focusing mechanism. In solids, the relative roles played by the Kerr effect and electrostriction have been the subject of much discussion.[131-140]

A. Track Formation Requires Self-Focusing Explanation

Track formation in optical glass by a ruby-laser beam was first reported by Hercher.[7] Observation of the phenomenon could hardly have been earlier, because a Q-switched laser is required to produce the effect. He described the damage as regions of gross fracture separated by lines of small bubbles collinear with the laser beam. At nearly the same time, Steinberg produced long tracks in optical quality borosilicate crown glass with a beam focused by a 46-cm focal length lens.[12] The tracks were up to several centimeters in length and a few micrometers in diameter. Later in the same year,[13,14] tracks were formed in fused silica and dense flint glass.

The straightness of the tracks and the length-to-diameter ratio rule out any explanation involving fractures or sparks propagating from a point. The

small track radius requires both self-focusing and filament formation. Without self-focusing the minimum beam radius in Steinberg's initial experiment is about 20 μm. This is too large a scale for the observed track radius. Self-focusing must maintain this radius over an appreciable length of the track. Without such filament formation, a beam only λ in diameter would spread out at a diffraction angle of about 60°. The track is explained as the residual damage after the high power of the laser beam is concentrated in such a small filament. As the filament leaves the exit face of the sample, it spreads through a very large angle by diffraction.

B. Role of Sound in Track Formation Process

Steinberg also observed an ultrasonic pulse which propagates transversely when the laser beam passes through a solid dielectric. The pulse was observed both above and below the threshold for damage. The pulse intensity was about the same for both ruby and sapphire samples, so absorption at the laser wavelength had little effect in creating the pulse.[12]

The fundamental wavelength of sound excited by the electrostriction is about equal to the beam diameter. For a 200 μm radius beam the sound frequency is about 10 MHz. Thus, the sound waves produced by electrostriction may be observed with an ultrasonic transducer.

Steinberg also observed a back-scattered pulse of stimulated Brillouin scattered light during track formation. The pulse had a shorter duration and faster rise time than the 55-nsec input laser pulse. The polarization was the same as the incident laser beam. The frequency shift corresponds to scattering from a longitudinal hypersonic wave having the same sound velocity as the transverse ultrasonic wave. The energy in the back-scattered pulse was quite low, indicating that the stimulated Brillouin scattering does not play a significant role in track formation.

C. History of Self-Focusing Theory

The first extended analyses of self-focusing also appeared in 1964. Chiao et al.[107] discuss steady-state laser-beam trapping for both liquids and solids. The critical trapping power was shown to be proportional to the optical wavelength squared, making it impossible to observe electromagnetic beam trapping except at optical wavelengths. In their analysis, the refractive index for the medium was expanded in terms of the electric field strength as

$$n = n_0 + \tfrac{1}{2} n_2 \langle E^2 \rangle$$

in cgs units as later corrected.[71] The coefficient n_2 was assumed to be due to either the Kerr effect or electrostriction in liquids, and to electrostric-

tion alone in solids. The trapping criterion used was derived from the critical angle for total internal reflection from a plane surface, and the diffraction angle for a beam passing through a uniformly illuminated aperture.

The subject of laser-beam trapping rapidly attracted the attention of many physicists. Kerr-effect self-focusing in liquids was soon well investigated experimentally.[58-98] Simultaneously, many theoretical physicists began analyzing steady-state beam trapping, using the above constitutive relation or extensions of it.[99-130] Several mechanisms for rapidly producing intensity-dependent refractive index changes were identified, including molecular reorientation,[107] microscopic clustering,[76] molecular libration,[90] and electronic polarizability.[63] All of these mechanisms are dependent only upon the local mean-squared electric field, and all are rapid compared with nanosecond laser-pulse rise times. Thus, they all scale the same way; all produce a threshold for self-trapping almost independent of beam diameter. While most authors followed Chiao et al. in acknowledging that the relaxation times for electrostrictive trapping were comparable to the pulse duration, no one seems to have attempted an analysis covering the transition between the transient and the steady-state regimes. Several authors compared the relative importance of Kerr effect and electrostriction for steady-state trapping in liquids.[131-140] The general conclusion was that Kerr effect predominates electrostriction in the steady state, and achieves even greater preponderance in the transient regime.

In solids, molecular reorientation and libration are frozen out. The magnitude of the molecular clustering effect has not yet been calculated for solids. The remaining Kerr effect due to electronic polarizability is quite small. Electrostriction is therefore the most likely mechanism for self-focusing of nanosecond pulses. As we shall see, the fact that the electrostriction relaxation time is comparable with the pulse duration helps to explain the dependence of the power threshold on laser-beam radius and pulse duration. The other local rapid effects cannot explain the large experimental variation of the threshold with beam radius because they all give a nearly constant power threshold for any radius initial beam.

D. Electrostrictive Self-Focusing Mechanism

A laser beam can propagate with a constant small diameter if the refractive index along the beam axis is greater than the refractive index of the surrounding medium. This is simply the principle of fiber optics or a light pipe. The beam is maintained in the filament by total internal reflection. Electrostriction increases the refractive index along the beam axis as follows. The electrostrictive force

in a homogeneous medium is the force on the medium which tends to draw the material into the region of high electric field. The electric field induces dipoles in the medium. A dipole aligned with a field will experience a force in a homogeneous medium proportional to the gradient of the square of the electric field, i.e., to the gradient of the intensity. The greatest magnitude of the force is found at about the half-width of the intensity distribution, that is, at the "edge" of the beam. Now consider differential elements of $r\,dr\,d\theta$ lying in a plane perpendicular to the beam axis. As the laser pulse rises, the force is suddenly applied to the differential elements, which were formerly at rest. Hence, for times short compared to the time required for sound to cross the beam radius, the displacement of the differential elements is inward and proportional to the force. It is easy to see that the innermost differential element is compressed. The next element is compressed on the right-hand side but decompressed on the left-hand side, so the net compression is less than the compression of the innermost element. The outermost element is actually rarefied. Thus the compression reaches a maximum on the beam axis. The refractive index is perturbed by an amount proportional to the compression.

A laser pulse of threshold power can therefore create its own waveguide and propagate without diffraction spreading. Laser pulses of more than threshold power will focus themselves to a smaller radius. At the smaller radius the intensity and the gradient both increase, so the electrostrictive force increases. This in turn leads to greater compression and therefore stronger focusing. Thus the laser beam will collapse to a very small diameter, limited by other processes.

When the beam has collapsed to a radius of a few wavelengths of light, the intensity is so high that many nonlinear effect may occur. The glass may be permanently damaged by such mechanisms as stimulated Brillouin scattering, nonlinear absorption of radiation, two- or three-photon absorption, electric breakdown, or generation of acoustic phonons. The threshold for track formation is not set by the threshold for any of these nonlinear effects. Rather, it is set by the threshold for self-focusing.

A more extensive qualitative explanation of the mechanism, including diagrams, has been published previously.[141]

E. Scope of Paper

An electrostrictive laser-beam self-focusing mechanism is analyzed theoretically here as the initiator of track formation in optical glass. This paper is limited to further mathematical elucidation of the self-focusing mechanism. No attempt will be made to determine what mechanism causes the permanent damage when self-focusing has made the intensity sufficiently high. Various damage mechanisms have been reviewed by Bliss.[142]

F. Plan of Paper

We will first discuss the light-sound coupling constant. Then we will derive the sound-wave equation for acoustic disturbances driven by electrostriction, and find a general solution and several specific solutions to within suitable approximations. Next, we will discuss propagation of a Gaussian beam as described by the beam-tracing equation.[143] The equation is solved for various cases of propagation through a homogeneous medium, and a medium where the refractive index has been disturbed by electrostrictively driven acoustic waves.

The theory of Secs. II and III is then applied to laser-beam self-focusing. A curve for the trapping threshold is obtained analytically for an approximate model. In the same model, the achieved intensity for a given laser pulse is obtained. A computer movie shows the development of the beam trajectory with time. Features shown by the movie help to explain the location of damage "stars" on the tracks. The results of the paper are compared with Steinberg's experimental data, and an attempt is made to characterize a failure intensity for the glass.

Results are summarized in Sec. V. The Appendix sets forth useful properties of Dawson's Integral. Table III represents a methodical search of the published literature describing laser-beam trapping effects for pulsed lasers in solids and liquids. Many of the relevant theoretical papers are also included.

II. RADIAL COMPRESSION WAVES DRIVEN BY LASER BEAM

Electrostrictive laser-beam trapping is caused by an interaction between light and sound. The strong electric field of the intense laser beam exerts an electrostrictive force on the material medium through which the beam passes. The force drives the sound wave. As the sound wave develops it alters the index of refraction of the medium. This in turn changes the trajectory of the beam and modifies the electrostrictive force.

In this section, we begin by deriving the light-sound coupling constant $\rho_0 \partial n/\partial \rho$ from the photoelastic properties. We then derive equations for the sound wave excited by a given laser-beam intensity distribution. We assume that the sound-wave amplitude is so small that the classical small-signal acoustic equations apply. Furthermore, we disregard all anisotropy of the medium, whether intrinsic or induced. This amounts to treating amorphous glass as a fluid. We seek solutions only for laser beams which are not too sharply focused, so that axial gradients of intensity are much smaller

than radial gradients. The laser beam will have a circularly symmetrical intensity distribution, although it may be either linearly or circularly polarized. Under these conditions, we may divide the beam axis into thin differential sections dz, and treat the sound wave as completely radial in each section.

The general solution we obtain is applicable in any given timestep, small compared with the time required for significant alteration of the beam trajectory. We use Hankel transforms to find the radial dependence of the sound wave as it propagates in the infinite medium. The time dependence of the solution for an arbitrary pulse shape is found using Green's functions. The on-axis sound-wave amplitude and its second radial derivative are calculated explicitly.

A. Value of Light-Sound Coupling Constant

Liquids. The value of the light-sound coupling constant $\rho_0 \partial n / \partial \rho$ may be found by several methods. For liquids, it is only necessary to differentiate the Clausius-Mosotti relation

$$\alpha / 3\epsilon_0 m = (n^2 - 1)/(n^2 + 2)\rho,$$

where the polarizability α per unit molecular weight m is assumed to be constant for small density changes. The formula is

$$\frac{\rho_0 \partial n}{\partial \rho} = \frac{(n_0^2 + 2)(n_0^2 - 1)}{6 n_0} .$$

This is called the Lorentz-Lorenz relation.

Experimental values for solids. Ritland has checked the validity of the Lorentz-Lorenz relation for samples of borosilicate crown glass whose density varied as a function of thermal history.[144] His experimental values differed from the Lorentz-Lorenz relation by 36%. However, the changes in density may have been accompanied by considerable local reordering, which would not occur under acoustic compression.

It is also possible to use values of $\rho_0 \Delta n / \Delta \rho$ measured under high hydrostatic pressure. These values usually differ considerably from those found by the Lorentz-Lorenz relation, because the molecular polarizability is not constant under high hydrostatic pressure. Furthermore, the condition of hydrostatic stress does not match the condition of electrostrictive stress caused by a gently focused laser beam, as we shall show.

Computed valves for solids. Under electrostrictive stress, we can show that the stress is two-dimentional for a circularly polarized laser beam. In this case, we may compute the light-sound coupling constant from the two photoelastic constants for an isotropic medium. First, we define the strain, permittivity, and relative impermittivity tensors in the standard way:

$$u_{ij} = \frac{1}{2} \left(\frac{\partial u_i}{\partial x_j} + \frac{\partial u_j}{\partial x_i} \right),$$

where (u_1, u_2, u_3) is the displacement

$$\epsilon_{ij} = \frac{\partial D_i}{\partial E_j}, \quad \left(\frac{\epsilon_0}{\epsilon} \right)_{ij} = \frac{\epsilon_0 \partial E_j}{\partial D_i} .$$

The index ellipsoid is defined as

$$x_i x_j \, (\epsilon_0 / \epsilon)_{ij} = 1.$$

It has the following property. Pass a plane through the origin of the ellipsoid, perpendicular to the propagation direction of the light beam. The intersection of the plane with the ellipsoid will be an ellipse. The two wavefronts which may be propagated through the medium in the given propagation direction will have refractive indices equal to the major and minor semiaxes of the ellipse. The displacement vector $\vec{D}$ corresponding to the higher refractive index vibrates along the major semiaxis.

For an undisturbed isotropic medium the index ellipsoid is spherical with a radius of n_0. The change in impermittivity with strain is given by the fourth-rank tensor p_{ijkl}. Nye[145] has shown that for small strains the impermittivity tensor takes the form

$$(\epsilon_0 / \epsilon)_{ij} = \delta_{ij}/n_0^2 + (p_{1111} - p_{1122})u_{ij} + p_{1122} u_{kk} \delta_{ij}$$

for an isotropic medium. The two independent photoelastic constants are often abbreviated p_{11} and p_{12}.

For a two-dimensional radial compression we have $d\rho / \rho = -u_{kk}$, and $u_{11} = u_{22} = -\frac{1}{2} d\rho / \rho$, while u_{33} and the off-axis components of the strain tensor are zero. This makes the impermittivity tensor diagonal. The intersection of the plane perpendicular to the z axis with the index ellipsoid is a circle. The refractive index along the x and y axes may be calculated as shown:

$$(\epsilon_0 / \epsilon)_{xx} = 1/n_x^2 = 1/n_y^2$$

$$= 1/n_0^2 - \tfrac{1}{2}(p_{11} + p_{12}) d\rho / \rho$$

$$= 1/(n_0 + dn)^2 \approx 1/n_0^2 - 2dn/n_0^3.$$

Comparison shows that the desired light-sound coupling constant is

$$\rho_0 dn / d\rho = \tfrac{1}{4} n_0^3 (p_{11} + p_{12}). \tag{1}$$

For three-dimensional stress (hydrostatic stress), the formula would be

$$\rho_0 dn / d\rho = \tfrac{1}{6} n_0^3 (p_{11} + 2p_{12}).$$

Radial compression from circularly polarized beam. We will now show that the electrostrictive compression is radial when the laser beam is circularly polarized and gently focused. Further, we will show that the strain induced by a plane-polarized gently focused laser beam cannot be described

as a compression.

We first obtain the permittivity tensor by taking the reciprocal of the relative impermittivity tensor. This is

$$\epsilon_{ij} = n_0^2 \epsilon_0 \delta_{ij} + n_0^4 \epsilon_0 [(p_{12} - p_{11})u_{ij} - p_{12}u_{kk}\delta_{ij}].$$

It is possible to derive the electric stress tensor from this expression, starting with a consideration of the free energy of a dielectric. A derivation is given in Landau and Lifshitz.[146] The electric stress tensor is

$$s_{ij} = \tfrac{1}{2}(n_0^2 + n_0^4 p_{11} - n_0^4 p_{12})\epsilon_0 E_i E_j$$
$$- \tfrac{1}{2}(n_0^2 - n_0^4 p_{12})\epsilon_0 E^2 \delta_{ij}.$$

While this formula was derived for the case of a static electric field, we may use it for the high-frequency light-wave electric field, provided we average the square of the field and use the refractive index n_0^2 instead of ϵ/ϵ_0, as above. The forces become the appropriate gradients of the average stress tensor:

$$f_i = \partial \langle s_{ij} \rangle / \partial x_j.$$

First consider the case of a circularly polarized beam, in which the electric field components are

$$E_1 = E_0 \cos \omega t, \quad E_2 = E_0 \sin \omega t, \quad E_3 = 0, \quad E_0 \propto e^{-2r^2/a^2},$$

and the scale of variation of a with respect to z is large compared with a. In this case the beam is gently focused so all gradients of the electric stress tensor with respect to z may be neglected compared with gradients with respect to x or y. This means there will be no need to compute such components as s_{13}, s_{23}, and s_{33}. For this case the average values of the first two diagonal components of the electric stress tensor are

$$\langle s_{11} \rangle = \langle s_{22} \rangle = \tfrac{1}{4} n_0^4 (p_{11} + p_{12})\epsilon_0 E_0^2,$$

while the average value of the only off-diagonal component of interest s_{12} is zero. We may write these results in terms of the light intensity, using the average value of the electric field energy:

$$I = \langle W_E \rangle \, 2c/n_0 = c\epsilon_0 n_0 \langle E^2 \rangle.$$

In this case,

$$I = c\epsilon_0 n_0 E_0^2.$$

Because the average values of s_{11} and s_{22} are equal, the force is isotropic. The only significant gradients of the light intensity are radial, so we obtain the isotropic radial force

$$f_r = c^{-1}(\tfrac{1}{4}n_0^3)(p_{11} + p_{12}) \frac{\partial I}{\partial r} = c^{-1} \rho \, \frac{\partial n}{\partial \rho} \frac{\partial I}{\partial r}.$$

An isotropic radial force of this distribution produces a two-dimensional compression. Comparison

with (1) shows we obtained the correct value of the light-sound coupling constant earlier.

Anisotropic forces from plane polarized beam. For the case of a plane polarized beam

$$E_1 = E_0 \cos \omega t, \quad E_2 = E_3 = 0,$$

the average electric stress tensor is also diagonal, with the elements

$$\langle s_{11} \rangle = \tfrac{1}{4}(n_0^2 + n_0^4 p_{11})\epsilon_0 E_0^2,$$

$$\langle s_{22} \rangle = \langle s_{33} \rangle = -\tfrac{1}{4}(n_0^2 - n_0^4 p_{12})\epsilon_0 E_0^2.$$

There will be no force in the z direction because the gradient of s_{33} is negligible. Because the first two stress tensor components are different, the forces in the x and y directions are unequal, so the electrostrictive force due to a plane-polarized beam is anisotropic. Both compressive and shear waves are generated, but the shear waves do not contribute to the self-focusing process. A self-focusing analysis for a plane-polarized beam would have to solve a vector sound-wave equation for the displacement. While the case is of considerable interest, it will not be pursued here. Experiments have shown self-focusing occurs with either linear or circular polarization. Furthermore, Steinberg showed that the exit beam is somewhat depolarized. Strong depolarization of the exit beam for filaments trapped in liquids was also observed by Close et al.[135]

B. Laser-Beam Intensity Distribution

The intensity distribution of a circularly symmetrical laser beam of the lowest-order transverse mode is

$$I(r, z, t) = W\pi^{-1}a^{-2}e^{-r^2/a^2}q(t), \tag{2}$$

where $a = a(z, t) =$ beam trajectory, $W =$ pulse energy, $q(t) =$ pulse shape, normalized so

$$\int_{-\infty}^{\infty} dt \int_0^{2\pi} d\theta \int_0^{\infty} r\,dr\, I = W.$$

In the absence of self-focusing, $a(z, t)$ becomes $a(z)$ only, and follows a hyperbolic path, as will be shown in Sec. IIIA. We assume in all cases that

$$\left| \frac{\partial a}{\partial z} \right| \ll 1,$$

signifying symbolically that axial gradients of intensity are much less than radial gradients.

C. Sound-Wave Equation

The small-signal classical acoustic wave equation for a fluid, relating the displacement $\vec{u}$ to the force density $\vec{f}$, is

$$M\nabla^2 \vec{u} + (\Lambda + M)\vec{\nabla}(\vec{\nabla}\cdot\vec{u}) - \rho_0 \frac{\partial^2 \vec{u}}{\partial t^2} = -\vec{f},$$

where Λ and M are the Lame elastic constants. Defining the compression $\sigma = - \vec{\nabla} \cdot \vec{u}$, taking the divergence of the above equation, and inserting the electrostrictive force given above, we obtain the compression sound-wave equation

$$\nabla_r^2 \sigma - \frac{1}{v^2} \frac{\partial^2 \sigma}{\partial t^2} = \frac{1}{cv^2} \frac{\partial n}{\partial \rho} \nabla_r^2 I.$$

Because the beam is not sharply focused, the only significant term of the Laplacian is the radial term

$$\nabla_r^2 = \frac{\partial^2}{\partial r^2} + r^{-1} \frac{\partial}{\partial r} .$$

Here the speed of a compression wave is

$$v = \left(\frac{\Lambda + 2M}{\rho_0} \right)^{1/2} .$$

The compression is just the fractional local increase in density, so it is proportional to the local increase in refractive index

$$n = n_0 + \rho_0 \frac{\partial n}{\partial \rho} \sigma.$$

We may therefore immediately write a refractive-index wave equation

$$\nabla_r^2 n - \frac{1}{v^2} \frac{\partial^2 n}{\partial t^2} = \frac{\rho_0}{cv^2} \left(\frac{\partial n}{\partial \rho} \right)^2 \nabla_r^2 I.$$

D. Hankel Transformation of Radial Dependence

Define the Hankel transform as

$$F(R) = \int_0^\infty r \, dr \, f(r) J_0(rR),$$

and its inverse as

$$f(r) = \int_0^\infty R \, dR \, F(R) J_0(Rr).$$

Integration by parts twice, using the Bessel function recursion relations, will show that

$$\int_0^\infty r \, dr \left(\frac{\partial^2 f}{\partial r^2} + r^{-1} \frac{\partial f}{\partial r} \right) J_0(rR) = - R^2 F(R).$$

The Gaussian is transformed as

$$\int_0^\infty r \, dr \, e^{-r^2/a^2} J_0(rR) = (\tfrac{1}{2} a^2) e^{-a^2 R^2/4} .$$

Define the Hankel transform of the refractive index change as

$$N(R, z, t) = \int_0^\infty r \, dr \, [n(r, z, t) - n_0] J_0(rR).$$

The refractive-index wave equation may now be transformed to

$$\frac{\partial^2 N}{\partial t^2} + v^2 R^2 N = \frac{W}{2\pi c \rho_0} \left(\rho_0 \frac{\partial n}{\partial \rho} \right)^2 R^2 e^{-a^2 R^2/4} q(t).$$

E. Piecewise-Linear Green's-Function Solution for Time Dependence

The refractive-index wave equation has now been reduced to a second-order ordinary differential equation. One important complication remains. The driving function is coupled to the time dependence of the beam tracing equation, through the beam trajectory a. The latter equation is nonlinear. To proceed, we may use a step-by-step solution. Choose a timestep Δt short compared with the time required for significant changes in the beam trajectory. Let there be n_t time intervals and $n_t + 1$ instants t_k, chosen so $t_0 = 0$ is the starting instant of the pulse and t_{n_t} is the ending instant. Also divide the axis into differential cross sections or slices Δz, short compared with the distance required for significant changes in the beam radius. Let there be n_z slices, delimited by $n_z + 1$ planes, z_j, chosen so that $z_0 = 0$ is the entrance plane, and z_{n_z} is the exit plane. We may then allow the beam radius to be constant, $a = a_{jk}$ for the jth slice of the beam and the kth interval.

First let us obtain the Green's-function solutions of

$$\frac{d^2 f}{dt^2} + \omega_0^2 f = \delta(t - t').$$

Multiply by $e^{i\omega t}$ and integrate from $t = -\infty$ to $t = +\infty$ to obtain

$$F(\omega) = e^{i\omega t'}/(\omega_0^2 - \omega^2).$$

The inverse Fourier transform

$$f(t) = \frac{1}{2\pi} \int_{-\infty}^\infty d\omega \, \frac{\exp[-i\omega(t - t')]}{\omega_0^2 - \omega^2}$$

may be evaluated by the theory of residues using contours which enclose the poles of the kernel for $t - t' > 0$. The result is

$$f(t) = \begin{cases} \sin[\omega_0(t - t')]/\omega_0 & \text{for } t - t' > 0 \\ 0 & \text{for } t - t' < 0. \end{cases}$$

Any arbitrary driving function may be considered to be a continuum of δ functions. Because of the linearity of the wave equation, the response may therefore be obtained by integrating the δ-function response for each element of the driving function. Thus, if the driving function were $Q(t)$, the response would be

$$f(t) = \omega_0^{-1} \int_{-\infty}^t dt' Q(t') \sin[\omega_0(t - t')].$$

For driving pulse shapes $Q(t)$ which have a definite

starting point $t = t_k$, we may reduce the range of integration, provided that we include the "position" and "velocity" attained by the end of the previous timestep. The solution becomes

$$f(t) = \omega_0^{-1} \int_{t_k}^{t} dt' Q(t') \sin[\omega_0(t - t')]$$

$$+ f(t_k) \cos[\omega_0(t - t_k)] + f'(t_k) \omega_0^{-1} \sin[\omega_0(t - t_k)].$$

The piecewise solution of the transformed refractive-index wave equation may now be written down by substitution. It is

$$N_{jk}(R, z, t) = \frac{W}{2\pi c \rho_0} \left(\rho_0 \frac{\partial n}{\partial \rho}\right)^2 \frac{R}{v} e^{-a_{jk}^2 R^2/4}$$

$$\times \int_{t_k}^{t} dt' q(t') \sin[vR(t - t')]$$

$$+ N_{j,k-1}(R, z, t_k) \cos[vR(t - t_k)]$$

$$+ \frac{\partial N_{j,k-1}(R, z, t_k)}{\partial t} \frac{\sin[vR(t - t_k)]}{vR}. \quad (3)$$

A similar formula for the time derivative may be obtained by differentiation with respect to t.

Once the integral has been evaluated for some suitable driving pulse shape $Q(t)$, formulas suitable for machine computations can be obtained. An integration over R from 0 to ∞ must be performed to invert the Hankel transform. We may divide the range into subranges ΔR delimited by points $R_0 = 0$, $R_1 = \Delta R$, through $R_{n_R} = n_R \Delta R$ for some suitable upper limit. Two arrays of size $n_R \times n_z$ must be reserved in memory to hold the positions $N_{j,k-1}$ and the velocities $\partial N_{j,k-1}/\partial t$. Initially the arrays are cleared to zeros, signifying that the medium is at rest before the start of the pulse. The positions and velocities are then revised at each timestep according to the above formula and its time derivative. The inverse Hankel transform is computed, and the resulting altered refractive-index distribution is used to compute the new beam trajectory. The computation has been carried out for some cases of interest, which will be described later.

Another approach is to proceed analytically a little farther and to invert the Hankel transform. This task is not as hopeless as it first appears, because of an important circumstance. As we will show in Sec. III B, to compute the trapping threshold the refractive-index distribution need only be found along the beam axis. Similarly, to solve the equation of motion of the beam trajectory we need only the second radial derivative of the refractive-index distribution along the beam axis. The choice of the beam axis as the line for computation reduces the integrals to easily evaluated forms. To see this, note that the refractive-index distribution is

obtained from the inverse Hankel transform as follows:

$$n_{jk}(r, z, t) = n_0 + \int_0^{\infty} R \, dR \, N_{jk}(R, z, t) J_0(Rr).$$

On the beam axis, where $r = 0$, the Bessel function $J_0(0) = 1$. Also, the second radial derivative may be evaluated by differentiating the Bessel function under the integral sign, assuming the usual physical conditions of interchangeability of differentiation and integration and using the recursion relations for derivatives of Bessel functions. Thus,

$$\frac{\partial^2 J_0(Rr)}{\partial r^2} = \frac{1}{2}[J_2(Rr) - J_0(Rr)]R^2,$$

$$J_2(0) = 0, \quad J_0(0) = 1.$$

The resulting distributions are

$$n_{jk}(0, z, t) = n_0 + \int_0^{\infty} R \, dR \, N_{jk}(R, z, t),$$

$$\frac{\partial^2 n_{jk}(0, z, t)}{\partial r^2} = -\frac{1}{2} \int_0^{\infty} R^3 \, dR \, N_{jk}(R, z, t). \quad (4)$$

We will presently show that these distributions have become Fourier sine transforms.

It is possible to reexpress the Hankel transform of the refractive-index solution in terms of a sum of the piecewise solutions. Use of this form will facilitate inverse Hankel transformation. Let us prove by induction that the following form is correct:

$$N_{jk}(R, z, t_{k+1}) = \left(\frac{WR}{2\pi c \rho_0 v}\right) \left(\rho_0 \frac{\partial n}{\partial \rho}\right)^2 \sum_{i=0}^{k} e^{-a_{ji}^2 R^2/4}$$

$$\times \int_{t_i}^{t_{i+1}} dt' q(t') \sin[vR(t_{k+1} - t')].$$

First of all, noting that

$$N_{j,-1} = \frac{\partial N_{j,-1}}{\partial t} = 0,$$

indicating that the medium is at rest, we find the expression is correct for $k = 0$. Next, assume the formula is correct for $k - 1$. The time derivative of the formula is easily found by differentiating with respect to t_k. Substituting this form in (3), and using the trigonometric formula

$$\sin(\alpha + \beta) = \sin\alpha \cos\beta + \cos\alpha \sin\beta,$$

one can easily show that the formula is correct for k. Therefore it is correct for all non-negative k. The on-axis refractive-index distribution and its second radial derivative may now be obtained by Fourier transformation, interchanging the order of integration on t' and R. The result is

$$n_{jk}(0, z, t_{k+1}) = n_0 - \left(\frac{W}{2\pi c \rho_0 v}\right)\left(\rho_0 \frac{\partial n}{\partial \rho}\right)^2$$

$$\times \sum_{i=0}^{k} \int_{t_i}^{t_{i+1}} dt' q(t') \left(\frac{d^2}{d(vt_{k+1} - vt')^2}\right)$$

$$\times \int_0^\infty dR \, e^{-a_{ji}^2 R^2/4} \sin[vR(t_{k+1} - t')].$$

A similar result holds for $\partial^2 n_{jk}(0, z, t)/\partial r^2$, except that the second derivative is replaced by one-half the fourth derivative in the above expression. The integral may be converted to a finite range by writing the sine as the imaginary part of an exponential to i times the same argument, completing the square in the expotential and shifting the variable. This makes the integral equal

$$(2/a_{ji}) \, D \left[(vt_{k+1} - vt')/a_{ji}\right].$$

We have used Dawson's integral

$$D(x) = e^{-x^2} \int_0^x e^{t^2} \, d\xi.$$

Refer to the Appendix for properties of this function and computer programs to evaluate it. The resulting formulas are now

$$n_{jk}(0, z, t_{k+1}) = n_0 - \frac{W}{\pi c \rho_0 v} \left(\rho_0 \frac{\partial n}{\partial \rho}\right)^2$$

$$\times \sum_{i=0}^{k} a_{ji}^{-3} \int_{t_i}^{t_{i+1}} dt' q(t') D'' \left(\frac{vt_{k+1} - vt'}{a_{ji}}\right),$$

$$\frac{\partial^2 n_{jk}(0, z, t_{k+1})}{\partial r^2} = - \frac{W}{2\pi c \rho_0 v} \left(\rho_0 \frac{\partial n}{\partial \rho}\right)^2$$

$$\times \sum_{i=0}^{k} a_{ji}^{-5} \int_{t_i}^{t_{i+1}} dt' q(t') D'''' \left(\frac{vt_{k+1} - vt'}{a_{ji}}\right). \quad (5)$$

This is the piecewise-linear Green's-function solution of the radial sound-wave equation. It requires knowledge of the beam trajectory at all the preceding time instants t_i. Further analytical progress can be made only by selecting the driving pulse shape.

F. Solution of Transformed Wave Equation for Various Pulse Shapes

Step-plus-ramp driving function. During any timestep, we may approximate the pulse shape $q(t)$ by the step-plus-ramp driving function

$$Q_k(t) = q(t_k) + [q(t_{k+1}) - q(t_k)](t - t_k)/\Delta t. \quad (6)$$

This gives a continuous approximation to the driving pulse, with a step-function derivative. Substitution and evaluation of the time integral yields the solu-

tion

$$N_{jk}(R, z, t) = \frac{W}{2\pi c \rho_0 v^2} \left(\rho_0 \frac{\partial n}{\partial \rho}\right)^2 e^{-a_{jk}^2 R^2/4}$$

$$\times \Big[q(t_k)[1 - \cos(vRt - vRt_k)]$$

$$+ \frac{[q(t_{k+1}) - q(t_k)]}{\Delta t}\left(t - t_k - \frac{\sin(vRt - vRt_k)}{vR}\right)\Big]$$

$$+ N_{j,k-1}(R, z, t_k) \cos(vRt - vRt_k)$$

$$+ \frac{\partial N_{j,k-1}(R, z, t_k)}{\partial t} \frac{\sin(vRt - vRt_k)}{vR} .$$

The formula for the time derivative may be found by differentiation.

δ *function.* The response to a single impulse or δ function $\delta(t)$ occuring at $t = 0$ will be

$$N_{j0}(R, z, t) = \frac{WR}{2\pi c \rho_0 v} \left(\rho_0 \frac{\partial n}{\partial p}\right)^2 e^{-a_{j0}^2 R^2/4} \sin vRt.$$

Parabolic pulse. Let the driving pulse shape be the single parabolic pulse

$$q(t) = \begin{cases} (3/2p)(t/p - t^2/2p^2), & 0 \leq t \leq 2p \\ 0 & \text{otherwise.} \end{cases} \quad (7)$$

The full width at half-maximum of this pulse is $2^{1/2}p$. The solution becomes

$$N_{j0}(R, z, t) = \frac{3W}{4p\pi c \rho_0 v^2} \left(\rho_0 \frac{\partial n}{\partial \rho}\right)^2 e^{-a_{j0}^2 R^2/4}$$

$$\times \left(\frac{t}{p} - \frac{t^2}{2p^2} + \frac{[1 - \cos vRt]}{v^2 R^2 p^2} - \frac{\sin vRt}{vRp}\right).$$

G. Solutions of On-Axis Refractive Index for Specific Driving Pulse Shapes

For simple driving pulse shapes with a finite number of nonvanishing derivatives, it is convenient to integrate the refractive-index formula by parts. This procedure may even eliminate the necessity for evaluating integrals. The on-axis refractive-index formula becomes

$$n_{jk}(0, z, t_{k+1}) = n_0 + \frac{W}{\pi c \rho_0 v} \left(\rho_0 \frac{\partial n}{\partial \rho}\right)^2 \sum_{i=0}^{k} \frac{1}{a_{ji}^3}$$

$$\times \left[\frac{a_{ji}}{v} q(t') + D\left(\frac{vt_{k+1} - vt'}{a_{ji}}\right)\right.$$

$$\times \left.\left(\frac{a_{ji}^2}{v^2} q'(t) - 2(t_{k+1} - t') q(t')\right)\right]$$

$$- \frac{a_{ji}^2}{v^2} \int D\left(\frac{vt_{k+1} - vt'}{a_{ji}}\right) q''(t') dt' \Bigg]_{t_i}^{t_{i+1}}$$

using $D'(\xi) = 1 - 2\xi D(\xi)$. The form given may be reduced for computation, or solved explicitly for certain pulse shapes.

Step-plus-ramp driving function. For general computation we may approximate the pulse shape as in (6). The refractive-index distribution becomes

$$n_{jk}(0, z, t_{k+1}) = n_0 + \frac{W(\rho_0 \partial n/\partial \rho)^2}{\pi c \rho_0 v}\left[\sum_{i=0}^{k} a_{ji}^{-3}(q_{i+1} - q_i)\frac{a_{ji}}{v}\right.$$

$$+ D\left(\frac{vt_{k+1} - vt_{i+1}}{a_{ji}}\right)\left((q_{i+1} - q_i)\frac{a_{ji}^2}{v^2} - 2(t_{k+1} - t_{i+1})q_{i+1}\right)$$

$$\left. - D\left(\frac{vt_{k+1} - vt_i}{a_{ji}}\right)\left((q_{i+1} - q_i)\frac{a_{ji}^2}{v^2} - 2(t_{k+1} - t_i)q_i\right)\right].$$

Here $q_i = q(t_i)$. All integration and differentiation is eliminated, making this formula very suitable for machine computation.

Rectangular pulse. For the single rectangular pulse

$$q(t) = \begin{cases} 1/p & \text{for } 0 \le t \le p \\ 0 & \text{otherwise} \end{cases}$$

a simple result may be obtained. Let the timestep Δt run from 0 to t, so only a single pulse is treated. The second subscripts on n and a may be dropped, and the sum covers only the zeroth term. Let $W/p = P$, the pulse power. First and second derivatives are zero, $t_1 = t$, $t_0 = 0$, and $q_1 = q_0 = 1/p$. The result is

$$n_j(0, z, t) = n_0 + \frac{2P(\rho_0 \partial n/\partial p)^2 t}{\pi c \rho_0 v a_j^3} D\left(\frac{vt}{a_j}\right). \quad (8)$$

Consider the solution at the end of the pulse, when $t = p$. The limiting behavior may be obtained from series expansion of Dawson's integral, and by the asymptotic expansion, as given in the Appendix. For short pulses or large beams we have the transient case:

$$\lim_{p\to 0} n_j = \lim_{a_j \to \infty} n_j = n_0 + N_T \frac{P(\rho_0 \partial n/\partial \rho)^2 p^2}{\pi c \rho_0 a_j^4},$$

where the factor $N_T = 2$.

For long pulses or small beams we obtain the steady-state case:

$$\lim_{p\to\infty} n_j = \lim_{a_j \to 0} n_j = n_0 + N_s \frac{P(\rho_0 \partial n/\partial \rho)^2}{\pi c \rho_0 v^2 a_j^2},$$

with the factor $N_s = 1$.

Triangular pulse. The leading edge of a tri-

angular pulse will excite the ramp response of a linear system. Let the pulse shape be

$$q(t) = \begin{cases} t/p^2 & \text{for } 0 \le t \le p \\ 2/p - t/p^2 & \text{for } p \le t \le 2p \\ 0 & \text{otherwise.} \end{cases}$$

The full width at half-maximum is p, just as in the case of the rectangular pulse, so the power P is W/p. The response during the first half of the pulse will be

$$n_j(0, z, t) = n_0 + \frac{P(\rho_0 \partial n/\partial \rho)^2}{\pi c \rho_0 v^2 a_j^2}\left[\frac{t}{p} - D\left(\frac{vt}{a_j}\right)\frac{a_j}{vp}\right]. \quad (9)$$

Consider the limiting behavior at the peak of the pulse, when $t = p$. The transient and steady-state cases are the same as before, except $N_T = \frac{2}{3}$, while $N_s = 1$.

Parabolic pulse. The parabolic pulse is very close to the Gaussian in shape, and has two continuous derivatives throughout its duration. Let the pulse be

$$q(t) = \frac{3}{2p}\left(\frac{t}{p} - \frac{t^2}{2p^2}\right), \quad q'(t) = \frac{3}{2p^2}\left(1 - \frac{t}{p}\right),$$

$$\quad (10)$$

$$q''(t) = -\frac{3}{2p^3}$$

during the interval $0 \le t \le 2p$, and let the pulse be zero otherwise. The full width at half-maximum is $2^{1/2}p$, so the power $P = W/2^{1/2}p$. The refractive index for a single parabolic pulse will be

$$n_j(0, z, t) = n_0 + \frac{3P(\rho_0 \partial n/\partial \rho)^2}{2^{1/2}\pi c \rho_0 v^2 a_j^2}$$

$$\times \left[\frac{t}{p} - \frac{t^2}{2p^2} - \frac{a^2}{vp} D\left(\frac{vt}{a_j}\right) + \frac{a^2}{v^2 p^2}\int_0^{vt/a_j} D(\xi)d\xi\right].$$

At the midpoint of the pulse we have $t = p$. The same transient response is obtained as for the rectangular and triangular pulses, except that $N_T = N_s = 3/2^{1/2} = 1.061$.

H. Solution of Second Radial Derivative of On-Axis Refractive Index

Step-plus-ramp drive. We will show in Sec. III that the most important case for a computer model of beam trapping is the second radial derivative of the on-axis refractive index for a step-plus-ramp driving function. Using integration by parts we may reduce (5) and (6) to

$$\frac{\partial^2 n_{jk}(0, z, t_{k+1})}{\partial r^2} = -\frac{W(\rho_0 \partial n/\partial \rho)^2}{2\pi c \rho_0 v^2}\sum_{i=0}^{k} a_{ji}^{-4}$$

$$\times \left\{ q_i D''' \left(\frac{vt_{k+1} - vt_i}{a_{ji}} \right) - q_{i+1} D''' \left(\frac{vt_{k+1} - vt_{i+1}}{a_{ji}} \right) \right.$$

$$+ \frac{a_{ji}}{v} \frac{(q_{i+1} - q_i)}{\Delta t}$$

$$\times \left[D'' \left(\frac{vt_{k+1} - vt_i}{a_{ji}} \right) - D' \left(\frac{vt_{k+1} - vt_{i+1}}{a_{ji}} \right) \right] \right\} .$$

The derivative relations and the program for $D(x)$ in the Appendix may now be used for computations. Only half as much storage is required as for the computation of the transformed wave equation.

Parabolic pulse. For a single parbolic pulse the second radial derivative of on-axis refractive index becomes

$$\frac{\partial^2 n_j(0, z, t)}{\partial r^2} = - \frac{3P(\rho_0 \, \partial n/\partial \rho)^2}{2^{1/2} \pi c \rho_0 v^2 a_j^4}$$

$$\times \left\{ \frac{t}{p} - \frac{t^2}{p^2} + \frac{a_j}{vp} \left[2 \left(\frac{vt}{a_j} \right)^2 + \frac{t}{p} - 1 \right] D \left(\frac{vt}{a_j} \right) \right\} .$$

$$(11)$$

This result is useful in certain approximate calculations. The quantity in braces may be expanded in a McLaurin series to obtain

$$\{ \cdots \} \approx 8v^2 t^3 / 3p \, a_j^2 .$$

Thus the response is initially proportional to the inverse sixth power of the beam radius. This proportionality dependence holds for any driving pulse shape except a δ function.

Rectangular pulse. The response to a single rectangular pulse is

$$\frac{\partial^2 n_j(0, z, t)}{\partial r^2} = - \frac{P(\rho_0 \, \partial n/\partial \rho)^2}{2 \pi c \rho_0 v^2 a_j^4} \left[2 \frac{vt}{a_j} D \left(\frac{vt}{a_j} \right) \right] .$$

As $t \to \infty$, the quantity in square brackets approaches 1. Thus the steady-state response is proportional to the inverse fourth power of the beam radius.

III. BEAM-TRACING EQUATION

The propagation, focusing, and deflection of a beam of Gaussian field distribution has been studied extensively. Normally such a beam spreads by diffraction, although the diffraction spreading is smaller than the spreading for any other field distribution. The spreading may be defeated by placing lenses periodically along the path of the beam, or by allowing the beam to propagate in a continuous inhomogeneous focusing medium. The trapping criterion gives the amount of focusing required to maintain the beam at approximately constant diameter. There is also a stability condition. If the beam is periodically refocused by means of thin lenses, the lens spacing divided by the focal length must be less than 4 for stable propagation.[147]

Pierce analyzed the propagation of a Gaussian beam in a homogeneous medium, starting with Maxwell's equations.[148] He showed that the beam retains its Gaussian intensity profile, and only the beam radius varies. Let the perpendicular distance from the propagation axis z to the point where the intensity drops to $1/e$ of the peak on-axis intensity be a, the beam radius. Then the beam trajectory will be the function $a(z)$. In a homogeneous medium, Pierce showed that

$$\frac{d^2 a}{dz^2} = \frac{\lambda^2}{(2\pi n_0)^2 a^3} .$$

This is the beam-tracing equation for a homogeneous medium.

The propagation of a Gaussian beam in inhomogeneous media has also been studied, subject to the paraxial-ray-tracing approximations of geometric optics.[143] The derivation started with the geometric optics ray-tracing equation and added Pierce's Gaussian beam expanding term, the right-hand side above. The new beam-tracing equation has a second term which characterizes the radial inhomogeneity:

$$\frac{d^2 a}{dz^2} = \frac{\lambda^2}{(2\pi n_0)^2 a^3} + \frac{a}{n_0} \left. \frac{\partial^2 n}{\partial r^2} \right|_{r=0} .$$

$$(12)$$

In the form shown here, we assume the inhomogeneity is azimuthally symmetric and collinear with the propagation axis. The collinearity assumption is certainly valid when the inhomogeneity is created by passage of the beam through a homogeneous medium. This equation may be used for the study of "large-scale" beam trapping, i.e., focusing of beams to diameters of many wavelengths. Essentially the same equation has been applied to the study of Kerr-effect trapping.[149]

The beam-tracing equation is analogous to the equation for the radial motion of a particle in a central field of force,[150] letting $a \to r$, $z \to t$, $k_0^2 n_0^2 \to m^2/l^2$, and all terms except the first $\to f(r)/m$ (choose $l = 1$). This analogy only holds, of course, if the second radial derivative of index is only a function of a, and not a function explicitly of z. A variety of solutions for different types of gravitational potentials may be transcribed as beam-tracing solutions. Homogeneous index corresponds to the force-free particle. Transient electrostrictive trapping in a section where the index change is uniform in z corresponds to a linear force.

A. Solution for Homogeneous Index

Hyperbolic trajectories. Let $a' = da/dz$. Then the beam-tracing equation becomes a differential equation in a alone:

$$\frac{1}{2}\frac{d(a')^2}{da} = a'\frac{da'}{da} = \frac{d^2a}{dz^2} = \frac{1}{k_0^2 n_0^2 a^3} = -\frac{1}{2k_0^2 n_0^2}\frac{d(a^{-2})}{da} .$$

This is easily integrated to give

$$(a')^2 + (k_0 n_0 a)^{-2} = C_1 .$$

The constant may be evaluated at the beam waist where $a = a_m$ and $a' = 0$, or at the entrance plane $z = 0$, where $a = a_0$ and $a' = a_0'$,

$$(a')^2 + (k_0 n_0 a)^{-2} = (k_0 n_0 a_m)^{-2} = (a_0')^2 + (k_0 n_0 a_0)^{-2} .$$

To obtain the z dependence, take the square root after transposing terms:

$$da/dz = a' = \pm (k_0 n_0)^{-1}(a_m^{-2} - a^{-2})^{1/2}$$

$$= \pm [(a_0')^2 + (k_0 n_0)^{-2}(a_0^{-2} - a^{-2})]^{1/2} ,$$

where the lower sign applies to a converging beam, and the upper to a diverging beam. Multiply through by $2a$ and rewrite as

$$dz = \frac{\pm k_0 n_0 da^2}{2(a^2/a_m^2 - 1)^{1/2}}$$

$$= \frac{\pm da^2}{2[(a_0')^2 a^2 + a^2/k_0^2 n_0^2 a_0^2 - 1]^{1/2}} .$$

Integration of the first form gives the ray path in coordinates centered at the beam waist where $z = z_m$. The formula may be written in the standard form for a hyperbola:

$$\frac{a^2}{a_m^2} - \frac{(z - z_m)^2}{k_0^2 n_0^2 a_m^4} = 1 .$$

The second form can be integrated to give the beam profile as a function of entrance conditions and z:

$$a(z) = [(a_0 + a_0'z)^2 + z^2/k_0^2 n_0^2 a_0^2]^{1/2} . \tag{13}$$

The slope at any point may now be given with no ambiguous sign. It is

$$\frac{da}{dz} = a^{-1}(z)\left((a_0 + a_0'z)a_0' + \frac{z}{k_0^2 n_0^2 a_0^2} \right) .$$

The distance to the beam waist for given entrance conditions may be found by setting the slope above equal to zero. This gives

$$z_m = \frac{-a_0 a_0'}{(a_0')^2 + 1/k_0^2 n_0^2 a_0^2} . \tag{14}$$

The distance is positive for an initially converging beam.

Beam radius produced by lens. For a beam of small half-angular divergence θ and radius a_0 incident on a thin lens of focal length f, the slope after passage through the lens is

$$a_0' = -a_0/f + \theta . \tag{15}$$

If the beam is collimated ($\theta = 0$), the distance to the beam waist is not f but

$$z_m = \frac{f}{1 + (f/k_0 n_0 a_0^2)^2} . \tag{16}$$

The beam radius at the beam waist becomes

$$a_m = \frac{f/k_0 n_0 a_0}{[1 + (f/k_0 n_0 a_0^2)^2]^{1/2}} . \tag{17}$$

In the above three formulas n_0 may be taken as 1 for air.

Invariance of a_m. In computing the beam waist radius in a glass sample of length L centered around the focus of an external lens, a correction may be made for the jump in refractive index when the beam is normally incident on the entrance face. Snell's law may be used to transform the ray slope at entrance. The steps are as follows:

(i) Compute z_m as above, with $n_0 = 1$;

(ii) Compute $a(z_m - \tfrac{1}{2}L)$, with $n_0 = 1$;

(iii) The angle of incidence θ_i is

$$\theta_i = \tan^{-1}\frac{f - (z_m - \tfrac{1}{2}L)[1 + (f/k_0 a_0^2)^2]}{f^2 a(z_m - \tfrac{1}{2}L)/a_0^2} ;$$

(iv) The angle of refraction is

$$\theta_r = (\sin\theta_i)/n_0;$$

(v) The entrance slope in the glass is

$$a'(z_m - \tfrac{1}{2}L) = -\tan\theta_r;$$

(vi) and the beam radius in the glass is

$$a_m = \frac{a(z_m - \tfrac{1}{2}L)}{\{1 + [k_0 n_0 a(z_m - \tfrac{1}{2}L)a'(z_m - \tfrac{1}{2}L)]^2\}^{1/2}} .$$

The correction will be very small unless θ_i is so large that $\sin\theta_i$ is not approximately $\tan\theta_i$. Otherwise, the reduction in slope is compensated by a reduction of the wavelength in the medium, and a_m remains unchanged.

Confocal parameter. The semiaxis b_0 of the hyperbolic path equals $k_0 n_0 a_m^2$. The intensity drops to one-half the waist intensity at this distance b_0 along the axis on either side of the beam waist. The length b_0 is termed the confocal parameter.[151] It is not invariant with change in index.

B. Solution for Kerr-Effect and Steady-State Electrostrictive Trapping

Geometric limit. A great deal of experimental and theoretical work has been done on Kerr-effect trapping. The properties of a medium whose refractive index may be characterized by $n = n_0 + \tfrac{1}{2}n_2$

$\times \langle E^2 \rangle$ (in cgs units) have been studied extensively and reviewed.[127] When we apply this refractive-index distribution to the large-scale beam-tracing equation we find a solution with an interesting geometric optics interpretation. The solution predicts the downstream motion of the focus during the rise of the pulse to the trapping threshold, but it does not give the correct value for the minimum beam-waist radius obtained above the trapping threshold.

The Kerr-effect constant n_2 is usually given in the cgs units cm sec^2/g; to convert to MKSA units, multiply by 10. The formula now becomes

$$n = n_0 + 2\pi n_2 \, \epsilon_0 \langle E^2 \rangle = n_0 + (2\pi n_2/cn_0) I \, ,$$

where I may be the Gaussian intensity distribution of (2). For convenience, we introduce the trapping parameter

$$T = 4Wq(t)n_2 k_0^2/c \, .$$

The beam-tracing equation then becomes

$$\frac{\partial^2 a}{\partial z^2} = \frac{1 - T}{k_0^2 n_0^2 a^3} \, . \tag{18}$$

The form of the equation is exactly the same as that for the homogeneous index case, provided we modify the wavenumber k_0. Introduce a pseudowavenumber and a pseudowavelength such that

$$1/\tilde{k}_0^2 = \tilde{\lambda}^2/4\pi^2 = (1 - T)/k_0^2.$$

Then as T approaches 1, the pseudowavelength approaches zero and the pseudowavenumber approaches infinity. In (16) and (17), as k_0 approaches infinity, the distance to the beam waist increases until it reaches the focal length of the external lens, while the beam-waist radius shrinks to zero. The beam envelope approaches a completely conical shape. This is exactly the geometric optics behavior expected if the wavelength of light were zero.

Above threshold the beam-tracing equation has no valid solutions. This may be seen from (13). A negative, zero, or complex value for a^2 would be nonphysical. In Eq. (13), a^2 is equal to a quadratic expression in z. For physical solutions, the quadratic expression must have no real roots, where a^2 would be zero. It will have no real roots as long as the discriminant $-4/k_0^2 n_0^2$ is negative. The discriminant is negative as long as T is less than 1. Thus, $T = 1$ is the trapping threshold. The trapping power is $P = c/4k_0^2 n_2$, which is a factor of $\pi/5.763 = 0.545$ less than that obtained by Garmire, Chiao, and Townes for a beam having a uniform intensity distribution.[71]

First integral and boundary conditions. The first integral is easily obtained, as before. For convenience let us first scale the radial and axial co-ordinates by measuring in units of $\lambda/2\pi n_0$. Then

$$A = k_0 n_0 a, \quad Z = k_0 n_0 z, \quad A' = \partial a/\partial z \, . \tag{19}$$

Use the chain rule for derivatives to obtain

$$A'' = A' \frac{dA'}{dA} = (k_0 n_0)^{-1} \frac{d^2 a}{dz^2} \, .$$

The beam-tracing equation may be integrated at once to give

$$(A')^2 + (1 - T)A^{-2} = C_1 \, .$$

In the usual experimental arrangement, an external lens focuses a nearly collimated laser beam into a sample of the medium centerd around the focus. "Focus" here means the low-power focus, before the beam power is so large that trapping effects occur. At low power the beam propagates as in a homogeneous medium. The waist radius a_m (or A_m) is the low-power minimum of the trajectory, and it occurs at z_m (or Z_m). The entrance conditions of the beam are fixed, whether the power is high or low, since the beam diameter at the external lens and at the entrance face of the sample is usually so large that the intensity threshold for non-linear effects is not achieved, even at high power. Then the entrance constant C_1 may be simply related to the low-power beam waist radius, as before:

$$C_1 = (A_0')^2 + A_0^{-2} = A_m^{-2}.$$

The second form is particularly convenient, as it permits choosing coordinates centered at Z_m, and leaves open the choice of sample length for the second integral.

Filament radius. The high-power minimum beam radius A_M may now be found by setting $(A')^2$ to zero (assuming $A_m \ll A_0$):

$$A_M^2 = (1 - T) A_m^2. \tag{20}$$

As we noted before, there are no valid solutions for $T \geq 1$.

General trapping criterion. The fractional increase in index on-axis is

$$\frac{\Delta n}{n_0} \equiv \frac{n|_{r=0} - n_0}{n_0} = \frac{2Wq(t)n_2}{cn_0^2 a^2}$$

in this case. The trapping condition $T = 1$, is seen to be equivalent to

$$\frac{\Delta n}{n_0} = \frac{1}{2k_0^2 n_0^2 a^2} \, ,$$

the general trapping criterion for Gaussian beams. The same result is obtained when the radial refractive-index inhomogeneity is uniform, as we will show later.

C. Solution for Inhomogeneous Index Caused by Electrostriction

Solving the beam-tracing equation for an inhomogeneous index distribution caused by electrostriction or thermal effects is much more difficult than solving the same equation for Kerr-effect trapping. In Kerr-effect trapping, the response of the medium to the electric field is virtually instantaneous, that is, very rapid compared to the rate of change of intensity in a nanosecond laser pulse. This makes it possible to relate the index inhomogeneity to the instantaneous local beam radius. Therefore we may separate the axial dependence z from the beam radius dependence a in the differential equation, and reduce the problem to quadratures. On the other hand, for effects such as electrostriction or thermal focusing and defocusing, the time lag for development of the effect leads to a dependence on the history of the beam radius. The leading edge of the laser pulse travels as a low-power beam would, along a hyperbolic path. This makes the initial beam radius distribution a hyperbolic function of z. As we showed at the end of Sec. II, the electrostriction effect leads to a refractive-index inhomogeneity which is initially proportional to the inverse sixth power of the beam radius. Therefore the effect is strongly localized initially around the low power focus. Because of this dependence, the order of terms in the beam-tracing equation is inverse third power and inverse fifth power. As the beam radius is always greater than a wavelength until a track is formed, we see that the inverse fifth power term is unimportant except for small radii.

If the pulse rises slowly enough and the pulse is long enough, a steady state is achieved. The electrostrictive effect goes as the inverse fourth power of the beam radius. It is therefore just like Kerr-effect trapping, and all the previous analysis applies to it. The steady-state condition might be achieved with long Q-switched laser pulses and sharply focused beams.

First integral. Measure distances in terms of $\lambda/2\pi n_0$ as in (18). A and Z are the scaled beam radius and axial coordinate. Let

$$F = -\frac{1}{k_0^2 n_0^3}\left.\frac{\partial^2 n}{\partial r^2}\right|_{r=0} .$$

Even though F is a function of Z, when we replace d^2A/dZ^2 with $A'dA'/dA$, we reduce F to the status of a parameter in the large-scale beam-tracing equation. The first integral, with the constant evaluated from the entrance conditions, is

$$(A')^2 + A^{-2} + FA^2 = C_3 \equiv (A_0')^2 + A_0^{-2} + F_0A_0^2 .$$

Second integral for axially uniform inhomogeneity.

The second integral cannot be performed in general when F is an arbitrary function of Z. In this case, the differential equation may not be cast into a variables separable form, and no integrating factors are known. However, in any short section of the beam path, we may consider F to be constant. (If the section is taken as the entire sample length, the meaning of the phrase "gently focused" becomes very stringent.) However, for such an axially uniform inhomogeneity, the equation may be solved.

Transpose, extract the square root, collect terms in A and Z, write dA as $dA^2/2A$, and obtain

$$\pm dZ = \tfrac{1}{2}dA^2\,(-FA^4 + C_3A^2 - 1)^{-1/2} ,$$

where the upper and lower signs correspond to an initially diverging or converging beam, respectively. For a real result, the integration range must be in the positive range of the radical. The two roots of the radical are

$$A_M^2 = \frac{C_3 - (C_3^2 - 4F)^{1/2}}{2F} , \quad A_N^2 = \frac{C_3 + (C_3^2 - 4F)^{1/2}}{2F} .$$

The integral may now be written

$$\pm (Z - Z_0) = \tfrac{1}{2}\int_{A_0^2}^{A^2} \frac{dA^2}{[-F(A^2 - A_M^2)(A^2 - A_N^2)]^{1/2}} .$$

Focusing medium. For the case of a focusing medium, F is positive. Stable propagation requires that F be no more than $\tfrac{1}{4}C_3^2$. Given this condition, both roots are positive. The integration range and conditions may be summarized by

$$A_N^2 > A^2 > A_M^2 > 0 \quad \text{for } \tfrac{1}{4}C_3^2 > F > 0.$$

Substitute

$$A^2 = C_3/2F + \sin\theta\,(C_3^2 - 4F)^{1/2}/2F ,$$

integrate, and solve to obtain

$$A^2 = \frac{C_3}{2F} + \frac{(C_3^2 - 4F)^{1/2}}{2F}$$

$$\times \sin[2F^{1/2}(Z - Z_0) + \sin^{-1}\psi] , \quad (21)$$

where

$$\psi = (2FA_0^2 - C_3)(C_3^2 - 4F)^{-1/2}.$$

As the range of the sine function is between -1 and $+1$, the maximum beam radius is A_N, and the minimum is A_M. The width of the minimum is much less than the width of the maximum, because A is the square root of the above expression. This behavior reflects the physical condition that the beam travels more slowly when it is concentrated in the high-index region near the axis, than it does when it is spread out.

Defocusing medium. When a powerful cw laser

beam passes through a liquid or gaseous weakly absorbing medium, thermal defocusing or blooming occurs. The same phenomenon can occur in a short section of a solid medium during transient electrostrictive focusing as follows. Let the leading edge of the laser pulse rise rapidly. The sudden onset of electrostrictive pressure drives the transient sound wave. Depending on the pulse shape and the dynamics of self-focusing farther upstream in the medium, as the sound wave propagates cylindrically away from the beam axis, it may leave a trailing wake with positive curvature of compression on axis. Therefore, for completeness, it is necessary to consider defocusing, where $F < 0$, even in the electrostrictive case.

For a defocusing medium there is no stability condition. The roots of the radical and the proper range of integration now obey the inequalities

$$A^2 > A_M{}^2 > 0 > A_N{}^2 \quad \text{for } F < 0 .$$

The integral is

$$\pm (Z - Z_0) = \tfrac{1}{2}(-F)^{-1/2} \ln \left[(-FA^4 + C_3 A^2 - 1)^{1/2} \right.$$

$$\left. + (\tfrac{1}{2} C_3 - FA^2)(-F)^{-1/2} \right]_{A_0{}^2}^{A^2} .$$

The explicit solution for A^2 is

$$A^2 = C_3/2F + \tfrac{1}{2}[(1 - C_3{}^2/4F)/\xi + \xi](-F)^{-1/2} ,$$

where

$$\xi = [(-FA_0{}^4 + C_3 A_0{}^2 - 1)^{1/2} + (C_3/2 - FA_0{}^2)(-F)^{-1/2}]$$

$$\times \exp[2(-F)^{1/2} (Z - Z_0)].$$

Basically, the beam diverges exponentially with distance, perhaps after a short section of initial convergence as may be caused by the entrance conditions. If there is a section of initial convergence, the minimum beam radius is A_M.

Trapping criterion. In a focusing medium, constant radius propagation can be achieved if the entrance slope is zero and if $C_3{}^2 = 4F$, so the coefficient of the sine term in (21) is zero. This also makes $A_M = A_N$. The condition on the radial inhomogeneity becomes $F = A_0{}^{-4}$ or

$$\frac{1}{n_0} \left.\frac{\partial^2 n}{\partial r^2}\right|_{r=0} = - \frac{\lambda^2}{(2\pi n_0)^2 a^4} ,$$

which just cancels the Gaussian beam diverging term in the large-scale beam-tracing equation.

We may relate this result to the previous trapping criterion. Since we have only the second radial derivative of the inhomogeneity evaluated on axis, we may choose the best-fitting parabolic inhomogeneity:

$$n(r) = n_0 \left(1 + \frac{r^2}{2n_0} \left.\frac{\partial^2 n}{\partial r^2}\right|_{r=0} \right)$$

$$= n_0 \left(1 - \frac{r^2 \lambda^2}{2(2\pi n_0)^2 a^4} \right) .$$

Now let Δn be $n(0) - n(a)$. Then

$$\frac{\Delta n}{n_0} = \frac{1}{2} \frac{\lambda^2}{(2\pi n_0 a)^2} , \tag{22}$$

exactly the trapping criterion derived before.

IV. MODEL SOLUTIONS FOR ELECTROSTRICTIVE LASER-BEAM TRAPPING

In this section we will use the previous results to discuss certain features of the trapping phenomenon. We will discuss the power threshold for trapping in both the transient and steady-state regimes of pulse duration versus beam size, for a simplified model. In the same model, we will calculate the maximum achieved intensity along the beam axis. A computer movie will show the development of the beam trajectory with time for a laser pulse at or near the threshold for trapping. We will discuss the variation of the self-focusing length with time, which produces upstream and downstream motion of the starting point of a track.

A. Transient and Steady-State Trapping Threshold

We have defined the self-trapping threshold as the amount of self-focusing required just to offset the tendency of a Gaussian laser beam to diverge. Further self-focusing leads to convergence and filament formation. During filament formation, the light-wave electric field increases dramatically. Within the filament, several nonlinear effects may occur. However, at the self-trapping threshold, the electric field intensity is not much greater than the intensity in the absence of self-focusing. This justifies our use of the small-signal acoustic wave equations in deriving the self-focusing threshold. The trajectory of a gently focused beam is substantially unaltered by self-focusing, up to the self-trapping threshold. On the other hand, once the self-trapping threshold is passed, the beam intensity increases rapidly in the propagation direction. Thus, downstream from the point where the self-trapping threshold has been reached, the trapping threshold is greatly exceeded. This process leads rapidly to filament formation. We may therefore calculate the self-trapping threshold by ignoring all changes of the trajectory until the sound wave is strong enough to cause self-focusing. The validity of this approximation depends on the strong nonlinearity of the beam propagation equation. Experimental justification for this approximation is found in the precipitous nature of self-focusing, as shown by the sudden change in exit beam divergence angle.

Under the above assumptions, the threshold may be calculated algebraically, using the specific result previously derived for the weak beam case. The general trapping criterion (22) gives the increase of refractive index on the beam axis required for trapping. Equation (8) gives the increase in refractive index $\Delta n = n_j - n_0$ for a rectangular pulse of power P. Solving for the pulse power gives the trapping threshold power

$$P_{\text{tr}} = \frac{c\lambda^2 \rho_0 v^2}{16\pi n_0 (\rho_0 \partial n/\partial \rho)^2 (vt/a_0) D(vt/a_0)} \quad .$$

Let us choose the pulse duration as the time $t = p$ when the sound waves have developed sufficiently to reach the trapping threshold. Any portion of the laser pulse occurring after this time will be trapped. We may collect most of the constant factors above in a single coefficient

$$K = \frac{c\lambda^2 \rho_0 v^2}{8\pi n_0 (\rho_0 \partial n/\partial \rho)^2} \quad . \tag{23}$$

This constant has the dimensions of power and is termed the trapping-power coefficient. The remaing factors in the power-threshold formula

$$P_{\text{tr}} = K/2(vp/a_0) D(vp/a_0)$$

are of the order of unity when $p \gtrsim a_0/v$. For short pulses or large beams we have the transient case

$$\lim_{p \to 0} P_{\text{tr}} = \lim_{a_0 \to \infty} P_{\text{tr}} = \frac{K}{N} \frac{a_0^2}{v^2 p^2} \quad ,$$

where the factor $N_T = 2$. Thus the transient case corresponds to an intensity threshold for fixed pulse duration. For long pulses or small beams we obtain the steady-state case

$$\lim_{p \to \infty} P_{\text{tr}} = \lim_{a_0 \to 0} P_{\text{tr}} = K/N_s \quad ,$$

where the factor $N_s = 1$.

Thus the steady-state case corresponds to a power threshold, and K is the steady-state trapping power.

Similar results may be derived for a triangular pulse or a parabolic pulse. From (9) we obtain the power-trapping-threshold formula for trapping at the peak of a triangular pulse,

$$P_{\text{tr}} = K/[1 - (a_0/vp) D (vp/a_0)].$$

The transient and steady-state cases are the same as before except that $N_T = \frac{2}{3}$, while $N_S = 1$. For the parabolic pulse, the power threshold from (10) is

$$P_{\text{tr}} = 2^{1/2} K/3 [\tfrac{1}{2} - (a_0/vp) D(vp/a_0)$$

$$+ (a_0^2/v^2 p^2) \int_0^{vp/a_0} D(\xi) d\xi] \quad .$$

Again the same transient response is obtained, ex-
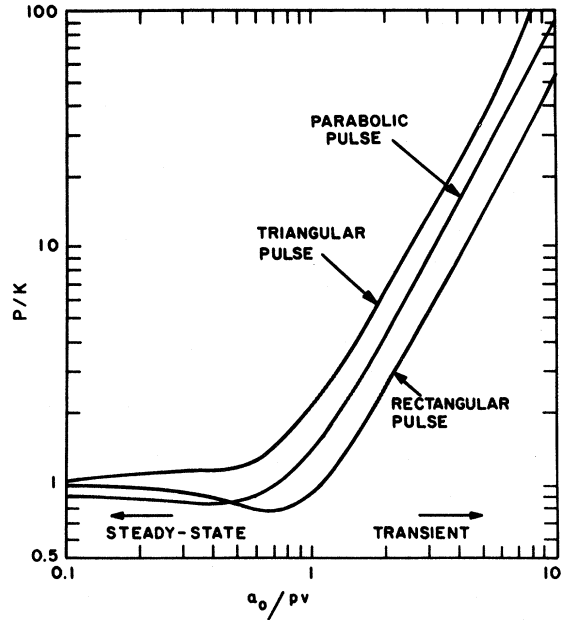
FIG. 1. Trapping threshold for three pulse shapes.

cept that $N_T = N_S = 3/2^{1/2} 2 = 1.061$.

The ratio of the time required for sound to cross the beam radius, a_0/v, to the pulse duration p determines whether the trapping threshold is a power threshold or an intensity threshold. The power-threshold case is the steady-state case, when the ratio drops to values below unity, for either small beams or long pulses. The intensity-threshold case is the transient case, where values of the ratio are larger than unity, for large beams or short pulses. The trapping threshold for the three pulse shapes is plotted as a function of the ratio in Fig. 1.

B. Evidence for Breakdown-Intensity Threshold

During track formation, a white flash of non-polarized light, similar in appearance to an air spark, is observed from the side of the sample. The white light comes from the entire length of the track.

The above fact suggests that electric field breakdown or multiphoton ionization causes the permanent damage in the track. If so, for a given pulse duration there should be a certain maximum light intensity the medium can withstand without damage. The relevant intensity, of course, is the maximum intensity achieved by the beam during the course of self-focusing. This intensity is not directly measurable. It must be calculated from the experimental pulse energy and pulse duration, and the theory of self-focusing.

C. Self-Focusing to Fixed Achieved Intensity

In the absence of self-focusing, the peak beam

intensity is achieved at the peak of the laser pulse and at the location of the beam focus. The intensity is calculated from the measured pulse energy, pulse duration, laser-beam angular divergence, and the focal length of the external lens, using (13)–(15). In a graph of the logarithm of pulse power versus the logarithm of beam size, the constant intensity lines are straight with a slope of 2.

When the beam power is large, self-focusing alters this picture significantly. As the beam focuses itself, the achieved intensity increases rapidly. The lines of constant intensity sag downward into curves. At very high intensities, the curves follow the trapping-threshold curve.

Constant achieved intensity curves for electro-strictive self-focusing may be calculated in the steady-state regime of long pulse duration and small beam radius. We have derived an expression for the beam radius achieved by a given amount of self-focusing. Also, we calculated the self-focusing coefficient for electrostrictive trapping, given a fixed beam radius and pulse shape. These results may be used in an approximate calculation. We will use the precipitous approximation of the previous model, in which we assume that the beam trajectory remains relatively undisturbed until self-focusing suddenly occurs. We also assume that in the region of the beam focus, the beam radius may be considered constant. We will use the steady-state results and extend them for some small distance into the transient regime. Finally, we will assume the peak achieved intensity occurs at the peak of the laser pulse. In spite of the many approximations involved, a useful result may be obtained.

The intensity is given by (2). Let us use the parabolic pulse (7) for the pulse shape $q(t)$. The achieved intensity on the beam axis at the peak of the parabolic pulse will be

$$I = 3\,W/2\pi p a_M^2 \;.$$

Defining the power as the pulse energy divided by the pulse full width at half-maximum gives

$$P = W/2^{1/2}p \;.$$

We may scale the high-power minimum beam radius a_M by the wavelength according to (19). Thus, the beam radius required to achieve a given intensity for a given beam power is

$$A_M^2 = 3\,k_0{}^2 n_0{}^2 P/2^{1/2}\pi I \;. \qquad (24)$$

The second radial derivative of the on-axis refractive index at the peak of a parabolic pulse is

$$\frac{\partial^2 n(0,z,p)}{\partial r^2} = -\,\frac{2^{1/2}3P(\rho_0\partial n/\partial\rho)^2}{\pi c\rho_0 v^2 a_m^4}\,\frac{vp}{a_m}\,D\!\left(\frac{vp}{a_m}\right)$$

from (11). This assumes the refractive-index distribution was established by the leading portion of

the pulse, on a length of the axis for which the beam radius does not differ greatly from a_m. We may insert this in (12). After simplifying the expressions using the scaling relations (19) and the trapping-power coefficient (23) we obtain the steady-state beam-tracing equation

$$\frac{d^2A}{dZ^2} = \frac{1}{A^3} - \frac{1}{A^3}\left\{\frac{2^{1/2}3}{4}\,\frac{P}{K}\left[2\,\frac{vp}{a_m}\,D\!\left(\frac{vp}{a_m}\right)\right]\right\}\;.$$

The term in square brackets approaches unity in the steady state. It thus becomes independent of the beam radius a_m. The above equation is now of the same form as (18), where the term in braces is equal to T. The relation between the high-power beam radius achieved by self-focusing and the low-power beam radius is given in (20). Equating this result with (24) gives the desired relation between the pulse power P and the low-power beam size. Solving, we have

$$P = \frac{\frac{1}{3}2^{1/2}}{1/\pi I a_m^2 + (vp/a_m)D(vp/a_m)/K}\;.$$

This equation has been plotted in Fig. 2 for several constant intensities. The achieved intensity may be compared with an electrostrictive trapping intensity given by
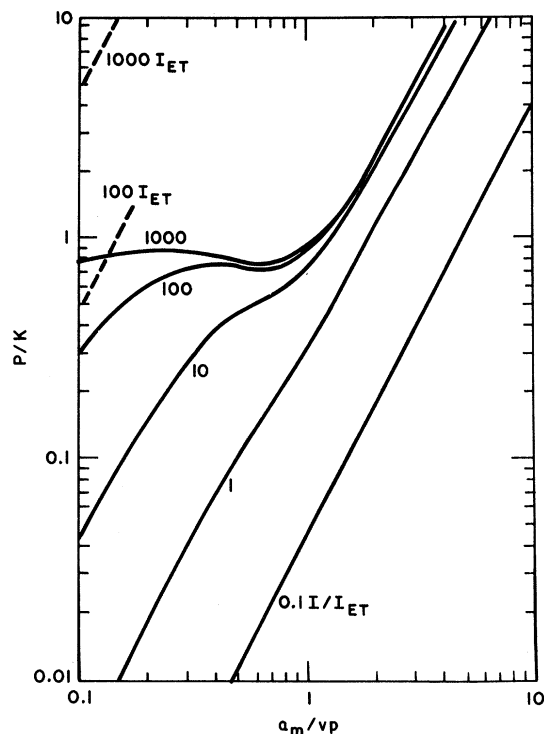
FIG. 2. Constant intensity curves for electrostrictive laser-beam trapping. Broken lines give power required to achieve the given intensity without trapping.

TABLE I. Physical properties of three optical glasses.

Property	Fused silica[a]	Borosilicate crown[b]	Dense flint[c]
Refractive index n at 694.3 nm	1.455 48	1.513 24	1.750 31
Density ρ (kg/m^3)	2200	2510	4720
Young's modulus Y (GN/m^2)	73.08	81.49	55.80
Modulus of rigidity M (GN/m^2)	31.16	33.73	22.36
Calculated Lamé elastic constant Λ (GN/m^2)	16.44	24.02	21.96
Calculated compression wave speed v (m/s)	5980	6037	3759
Measured $\rho_0 \, \Delta n/\Delta\rho$	0.29[d]	0.27[e]	
Trapping-power coefficient K using above (kW)	3697	4768	
Calculated $\rho_0 \partial n/\partial\rho$ (Clausius-Mosotti)	0.527	0.609	0.995
Trapping-power coefficient K using above (kW)	1119	937	221

[a]Engelhart Suprasil I.

[b]Schott BK-7.

[c]Schott SF-55.

[d]R. M. Waxler et al., J. Res. Natl. Bur. Std. (U.S.) 69A, 325 (1965).

[e]R. M. Waxler (private communication).

$$I_{\rm ET} = K/\pi(vp)^2 , \qquad (25)$$

the intensity (without self-focusing) of a beam having the trapping-power coefficient as its power and a pulse duration equal to the time required for sound to cross the beam radius. For $I \leq I_{\rm ET}$, self-focusing is weak. The achieved intensity is equal to the intensity calculated without self-focusing. When $I \gg I_{\rm ET}$, self-focusing greatly reduces the power required to achieve a given intensity. In the limit of higher and higher achieved intensities, in the transient regime, it appears that the power required is set by the threshold for trapping rather than by the desired intensity. We must not try to extend this result too far into the transient regime, as it depends on a steady-state trapping formula. We may expect the true achieved intensity curve to rise more rapidly in the right-hand side of Fig. 2 than our approximate solution indicates.

If $(vp/a_m)D(vp/a_m)$ is replaced in the above equation by its steady-state value of $\frac{1}{2}$, we obtain an equation similar in form to one derived by Zverev.[20] He attributes the self-focusing to a combination of thermal trapping and electrostriction. In the case where the absorption coefficient of the medium is very small, electrostriction is dominant over thermal trapping.

D. Numerical Comparison with Experimental Track Formation Thresholds

The theory may be compared with Steinberg's experimental track formation thresholds.

Table I lists the known physical properties of the three optical glasses tested by Steinberg. As we noted earlier, the value of the trapping-power coefficient varies widely depending on the value of the light-sound coupling constant used. For consistency, we have used the values obtained by the Clausius-Mosotti relation. These values produce the best agreement of the theory with experiment.

The trapping threshold and a curve of constant intensity are plotted for each of the three test glasses in Figs. 3–5. In each figure, the broken-line curve is the trapping threshold for a parabolic pulse, using the value of K indicated. The change in slope of the curve occurs approximately at the low-intensity beam radius equal to vp. In the experiments, the pulse full width at half-maximum was 55 nsec, so $p = 39$ nsec. The solid curve gives the power required to achieve the indicated fixed intensity with the aid of self-focusing. The value of the intensity was chosen to give a good fit to the experimental data points. Each circle on the figures represents a single experiment in which a laser pulse passed through the glass sample. If no track was produced, the circle is open; otherwise, it is
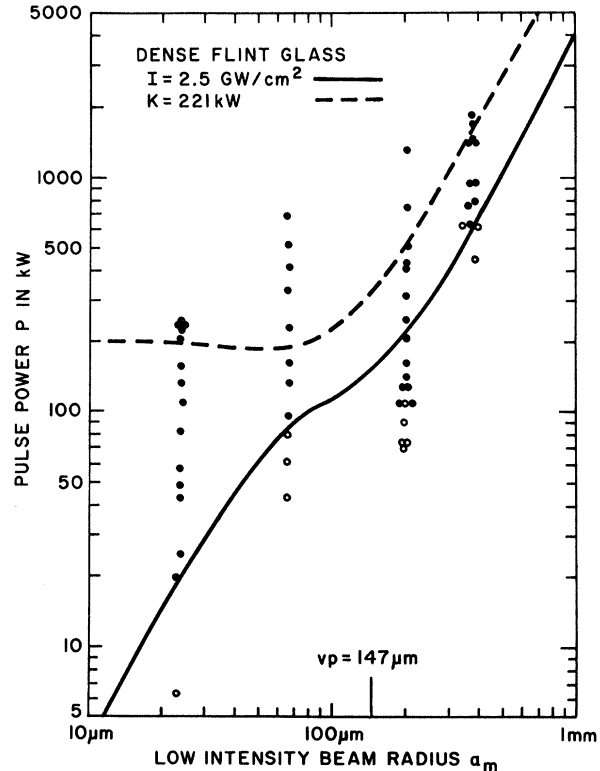
FIG. 3. Track-formation thresholds in dense flint glass. The threshold lies between the solid and open circles, which represent track formation and no damage, respectively.
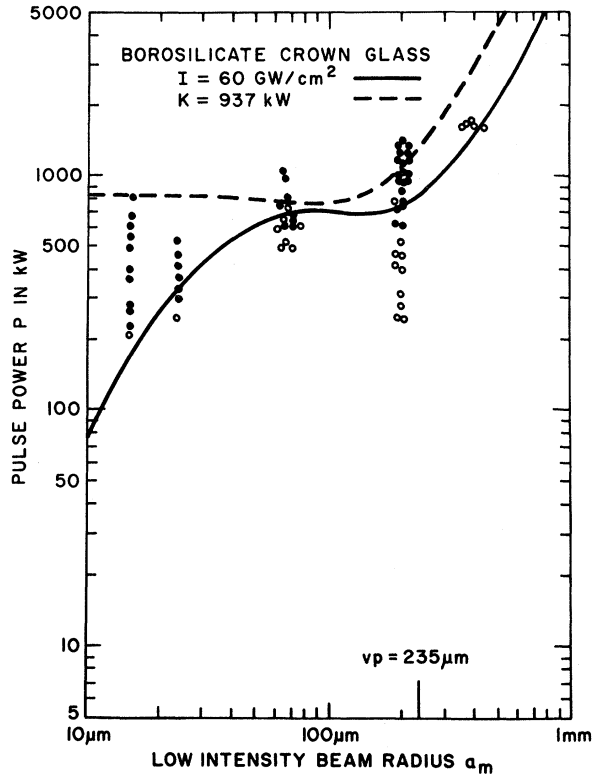
FIG. 4. Track-formation thresholds in borosilicate crown
glass.

filled. Thus, the experimental threshold lies be-
tween the lowest filled circle and the highest open
circle at each beam radius. The beam radii were
calculated from the lens focal length, the known di-
vergence of the laser beam, and the beam radius at
the external lens according to the analysis presented
earlier.

A summary of the thresholds of self-focusing pa-
rameters for the three glasses is given in Table II.

The worst disagreement between theory and ex-
periment is about a factor of 2 for dense flint glass
at 200 μm beam radius. At all other points, this
agreement is much closer. We note that in the
transient regime, to the right of the figures, the
constant intensity curve should probably rise more
sharply to give better agreement with experiment.
This may be due to our extension of the steady-
state beam-tracing solution into the transient re-
gime. In view of the many approximations required
to obtain a theoretical model, the agreement is
satisfactory.

E. Computer Movie of Beam Trapping

Beam trapping is caused by the interaction of
light and sound waves. In Secs. IV A and IV C, we
have obtained results analytically only by ignoring
most of the interaction. We assumed the beam tra-

jectory was not significantly altered during the first
portion of the laser pulse. We also considered only
a slice of the beam so short that the beam radius
was approximately constant in it. Under these as-
sumptions, the driving term of the sound-wave equa-
tion had a constant dimensional scale, the beam
radius. After the sound-wave amplitude had in-
creased sufficiently, we computed its effect on the
beam radius, using the beam-tracing equation for
an axially uniform medium. Considering the beam
radius to be constant in space and time until it
changes suddenly may seem to be a drastic approxi-
mation, but fortunately it produces good results.
The accuracy of the results has been checked by
computation.

Method of Computation. First, we replace the
precipitous self-focusing approximation and the ap-
proximation of beam radius constancy in the focus
region by the stepwise interaction and axial slice
approximation. The beam axis was divided by 101
transverse planes into 100 slices each 0.125 cm
thick. The pulse duration was also divided at 101
time instants into 100 time intervals. The computa-
tion proceeded in steps as follows:

(i) The initial time instant was $t_0 = 0$.

(ii) The beam radius was computed at each trans-
verse plane along the axis. In this computation, the
beam-tracing equation was solved by a standard
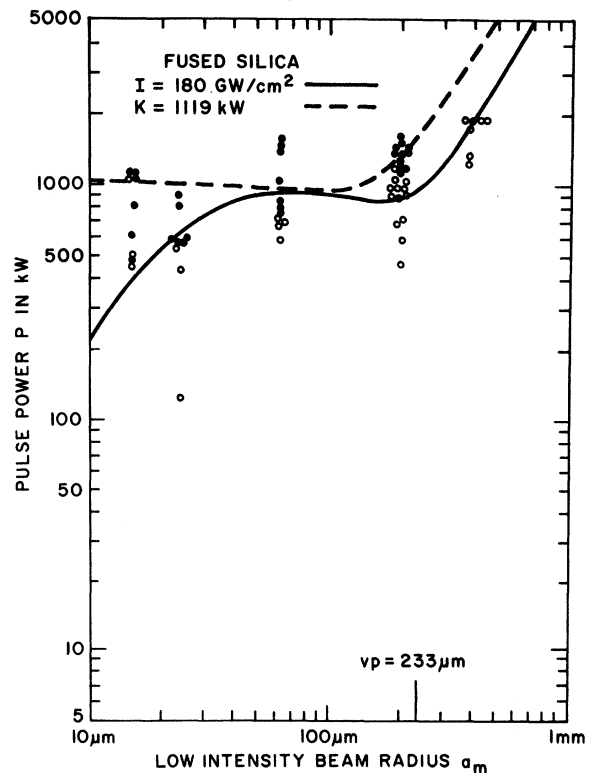
FIG. 5. Track-formation thresholds in fused silica.

TABLE II. Thresholds for three optical glasses.

Parameter	Fused silica	Borosilicate crown	Dense flint
vp (μm)	233	235	147
K (kW)	1119	937	221
I (GW/cm^2)	180	60	2.5
I_{ET}(GW/cm^2)	0.66	0.54	0.33
I/I_{ET}	274	111	7.68

Runge-Kutta method, using values of the second radial derivative of refractive index for each trans-verse plane along the axis. (At the first time instant the second radial derivative of refractive index was zero everywhere along the axis, since the medium was at rest.) We chose a fixed entrance beam radius of 0.1 mm, and an entrance slope of -0.001839 (at the first time instant, without self-focusing, the beam followed a hyperbolic trajectory with a minimum beam radius a_m of 0.05 mm.)

(iii) We computed the Hankel transform of the refractive-index change N_{jk} from (3). The pulse shape used was the step-plus ramp approximation (6) to a quartic pulse

$$q(t) = \begin{cases} (15/16p)(t/p)^2(2-t/p)^2 & \text{for } 0 \le t \le 2p \\ 0 & \text{otherwise} . \end{cases}$$

The full width at half-maximum of this pulse is

$$(4 - 2^{1/2}2)^{1/2}p = 1.082p .$$

The initial values of the "position" for the jth trans-verse plane, $N_{j,-1}$, and the "velocity", $\partial N_{j,-1}/\partial t$, were zeros for all the planes. The positions and velocities were computed for forty values of R, from 5 mm^{-1} to 200 mm^{-1} in steps of 5 mm^{-1}.

Note added in proof. The upper limit of 200 mm^{-1} is adequate for an initial minimum beam radius of 50 μm. As the minimum beam radius drops dynamically to as little as 5μm the upper limit should have been 2000 mm^{-1}. Computer memory limitations prohibited such a high upper limit. The effect of the low upper limit was to artificially attenuate the small-wavelength sound wave, which prevents small filament formation in the computed results. Current computations using the results of Sec. II H transcend this limitation and do show filament formation. Details are to be published as soon as the results are checked.

(iv) Equation (4) was used to compute the second radial derivative of the refractive index at each plane along the axis. The integral from 0 to ∞ was replaced by a Simpson integral over the forty position values previously computed.

(v) The time variable was advanced by 0.02 of the pulse duration. When the time became greater

than the pulse duration, we stopped. Otherwise, we returned to step (ii).

At the zeroth timestep and every tenth subsequent timestep the beam trajectory was plotted. The resulting 11 plots form a movie of 11 frames. Each frame is a snapshot of the beam trajectory over an axial length of 12.5 cm from the entrance face.

Features shown by the movie. A movie for a typical case of beam trapping is shown in Fig. 6. The beam enters from the left-hand side, with an entrance radius and slope fixed by an external lens. Note that the horizontal scale is compressed 100 times relative to the vertical scale. The case chosen was $\lambda = 1$ μm, $n_0 = 1.5$, $a_0 = 100$ μm, $a_0' = -0.001839$, $a_m = 50$ μm, $vp/a_m = 0.7$, and $P = 3K$. The beam power is considerably above the trapping threshold power, and the pulse duration is long enough so the steady-state features will be seen.

The first frame shows the hyperbolic beam tra-jectory taken by the weak leading edge of the laser pulse. The sixth frame corresponds to the peak of the laser pulse, and the eleventh frame gives the beam trajectory at the trailing end of the laser pulse. Initially, in frame 1 there is only one focus point. As the sound wave begins to build in inten-sity, the initial focal point moves upstream as seen in frames 2–4. The focal point moves upstream because the glass acts as an acoustic lens of in-
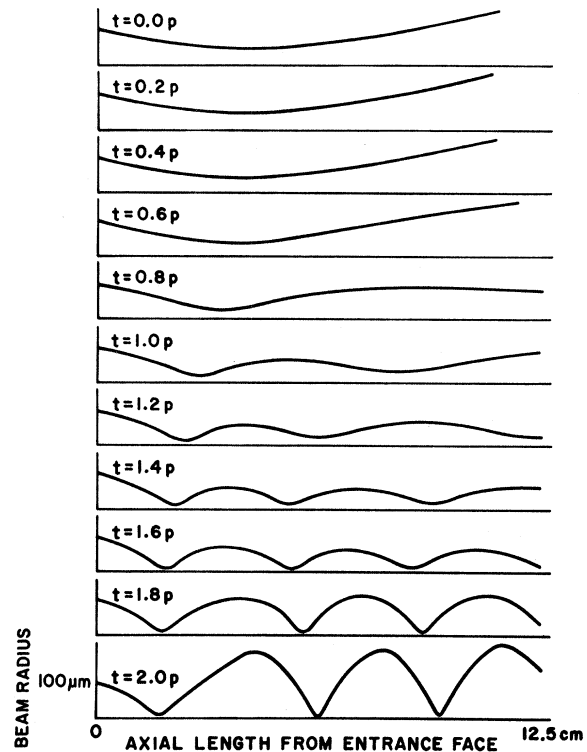
FIG. 6. Computer movie of electrostrictive laser-beam trapping.

creasing strength and decreasing focal length. By
the fifth frame the focusing strength of the sound
waves near the initial focus has increased enough
to bring the beam to a second focus farther down-
stream. By the sixth frame this second focus has
also moved rapidly upstream. The whole beam
reaches a relatively constant small radius for a
considerable distance along the axis, just as the
laser pulse is at the peak. We note that the onset
of trapping was quite sudden, between the fourth
and fifth frames.

As the laser pulse dies away in the seventh
through eleventh frames, the focal points continue
to move upstream. Eventually, at the end of the
pulse, the third focal point begins to move down-
stream again. Of particular interest is the long
period of time the focal points dwell at the upstream
ends of their range of motion. The first focal point
stays in almost the same position for the last third
of the pulse. At the very end of the pulse, the re-
gions which earlier formed the strongest acoustic
lenses have already relaxed and become diverging
lenses, while the regions between them are ap-
proaching their maximum focusing power. The net
result is several regions of sharp focus separated
by regions of large beam radius.

Between the fifth and tenth frames the first focus
moves upstream a distance of about 350 a_m in a time
$1.0p = 0.7 \, a_m/v$. Thus the speed is about 500 times
the speed of sound. Probably the speed would be
slower for a more sharply focused beam. The
speed and upstream propagation have been con-
firmed by two experiments.[4,152]

F. Dynamic Explanation for Location of Damage Stars

Steinberg investigated several dynamic aspects
of the track formation phenomenon. Near the
threshold power, the starting point of the track was
found near the focal point of the external lens. As
the power level was raised above threshold, the
track starting point was found farther and farther
upstream, but always a centimeter or so down-
stream from the entrance face of the sample. This
same result was reported by Zverev.[16] A particular
feature of the damage noted by Hercher and Stein-
berg was the appearance of gross regions of frac-
ture, called damage stars, usually at the upstream
ends of the tracks. Using filters, Steinberg showed
that laser light is side-scattered during track for-
mation, but only from the points where the damage
stars are found. This indicates that the fracturing
of the damage stars occurs before the end of the
laser pulse.

The track cannot start at the entrance face of the
sample, because some initial length of the sample
must serve as the region in which self-focusing
occurs. Clearly, track formation must occur before
the damage stars are developed. Otherwise, the

damage stars would scatter the laser beam at wide
angles, and cast a shadow over the region of the
track. As the computer movie shows, the beam
first becomes self-focused into a filament. Sharp
foci, moving rapidly upstream, appear later. These
foci dwell for a relatively long time at the upstream
ends of their motion. The high electric fields at
the foci cause the most extensive destruction there.

G. Depolarization of Light in Filament

The transmitted light is depolarized as a function
of azimuth during trapping of a linearly polarized
beam (Paper I, Fig. 12). The effect is apparently
explained by a third term which appears in the vec-
tor light-wave equation when refractive-index in-
homogeneities exist in the medium. Under these
conditions, the vector light-wave equation is

$$\nabla^2 \vec{E} - n^2 c^{-2} \frac{\partial^2 \vec{E}}{\partial t^2} = -\vec{\nabla}(\vec{E} \cdot \vec{\nabla} \ln n^2) \ .$$

The term on the right-hand side is significant only
when the scale of variation of the refractive index
is comparable to a wavelength of light. This condi-
tion occurs during track formation in glass, as the
beam diameter also approaches a wavelength of
light. The term provides coupling between the Car-
tesian components of the electric field. Thus it
tends to depolarize a linearly polarized beam.

Let the incident laser beam be linearly polarized
along the x direction, so

$$E_x = E_0 \cos \omega t, \quad E_y = E_z = 0 \ .$$

Let a polarizer be placed at the exit face of the
sample, with its axis in the y direction. During
track formation, the intensity in the center of the
filament is high, and the polarizer leaks enough
light to expose the central region of the photograph.
An interesting effect occurs at the edges of the
beam, where the intensity is weaker. On either
side of the beam, along the x axis, the gradient of
refractive index has only an x component. The dot
product of this with E_x is therefore nonzero, but
the gradient of this dot product again only has an x
component. The right-hand side of the above equa-
tion therefore does not couple energy into E_y, so
there is no depolarization and no light is transmitted
through the polarizer.

Now consider the regions above and below the
filament, on the y axis. Here the refractive-index
gradient only has a y component, so the dot product
with E_x is zero. Again there is no depolarization
of the light-wave field.

Finally, consider the areas on the beam perimeter
which do not lie close to either the x or y axis. In
these areas the refractive-index gradient does have
an x component, so the dot product with E_x is non-
zero. Also, the gradient of the dot product has a y
component. Therefore, in these regions there is

coupling into the E_y component. The resulting depolarized light is transmitted by the polarizer. This explains the peculiar cross-shaped pattern of light photographed by Steinberg.

V. CONCLUSIONS

An electrostrictive mechanism has been shown to be a cause of track formation by Q-switched lasers in optical glass. The mechanism involves an ultrasonic radially propagating sound wave excited through electrostriction, and beam focusing by the sound-wave compression.

Electrostriction can produce an acoustic lens to self-focus the laser beam, even in times short compared with the relaxation time. The self-focusing causes the laser beam to collapse to a small radius and to achieve high intensities. At the high intensities, the thresholds for many nonlinear effects may be exceeded. Thus, the actual cause of damage associated with track formation is not identified, but the track formation threshold depends on the self-focusing or trapping threshold rather than on the intensity threshold for any given nonlinear phenomenon.

We obtained the electrostrictive trapping threshold power as a function of beam radius and pulse duration for three pulse shapes. Given the wavelength, beam radius, pulse duration, and pulse shape, the trapping threshold may be computed for any isotropic material for which the density, speed of compressional sound waves or elastic moduli, and refractive index at the laser wavelength are known.

We also gave a formula for the power required to achieve a given maximum intensity, as a function of beam radius and pulse duration. The family of curves for different intensities may be classified in two groups. If the desired constant intensity is small compared with the electrostrictive trapping intensity defined in (25), no self-focusing effects occur, and the power required may be computed from the given intensity and the beam radius. If the desired intensity is large compared with the electrostrictive trapping intensity, self-focusing greatly reduces the power required to achieve the given intensity.

A comparison of the trapping threshold and a fitted value of the intensity threshold with experimental track-formation thresholds for each of three glasses showed substantial agreement.

A computer movie of beam trapping was presented. The computation fully included the interaction effects between light and sound. The movie showed the self-focusing of the beam to a relatively constant small radius throughout its length. It also showed the upstream motion of the focal points during the trailing part of the pulse, with a speed greatly exceeding the speed of sound. The focal points dwell for a considerable length of time at the upstream end of their range of motion, and may then recede downstream.

ACKNOWLEDGMENTS

APPENDIX: DAWSON'S INTEGRAL

Definition.

$$D(x) = e^{-x^2} \int_0^\infty e^{t^2} d\xi .$$

Fourier transform representation.

$$D(x) = \int_0^\infty \tfrac{1}{2} e^{-t^2/4} \sin\xi x \, d\xi .$$

Relation to error function.

$$D(x) = (i\tfrac{1}{2}\pi^{1/2}) e^{-x^2} \text{erf} ix .$$

Derivatives.

$$D' = 1 - 2xD ,$$
$$D'' = -2x + (4x^2 - 2)D ,$$
$$D''' = 4x^2 - 4 + (12x - 8x^3)D ,$$
$$D'''' = 20x - 8x^3 + (12 - 48x^2 + 16x^4)D .$$

McLaurin series expansion.

$$D \cong x - \tfrac{2}{3}x^3 + \tfrac{4}{15}x^5 - \cdots .$$

Asymptotic expansion.

$$\lim_{x\to\infty} D = -i\tfrac{1}{2}\pi^{1/2} e^{-x^2}$$
$$+ \frac{1}{2x}\left(1 + \frac{1}{2x^2} + \frac{1.3}{(2x^2)^2} + \frac{1.3.5}{(2x^2)^3} + \cdots\right) .$$

Limiting behavior.

$$\lim_{x\to\infty} 2xD = 1 .$$

Dawson's approximation.

$$2\pi^{1/2} e^{x^2} = 1 + 2\sum_{n=1}^\infty e^{-n^2/4} \cosh nx ,$$

relative error $< 2\times 10^{-17}$.

Computing method.

$$D(x) = (1/2\pi^{1/2})$$

$$\times \left\{ x e^{-x^2} + \sum_{n=1}^{\infty} \exp[-(x - \tfrac{1}{2}n)^2]/n - \exp[-(x + \tfrac{1}{2}n)^2]/n \right\}.$$

For negative x, use $D(-x) = D(x)$. To prevent underflow, do not compute the first term if $x \geq 6$. Compute the first term of the sum from 1 through the greatest integer $\leq 8 - 2x$, and not at all if $8 - 2x < 1$. Compute the second term of the sum from the maximum of 1 and the greatest integer $\leq 2x - 8$, through the greatest integer $\leq 2x + 8$.

A FORTRAN subroutine based on this method gave the same result ± 0.00002 as Abramowitz and Stegun.[153]

Integral. An approximate formula for the integral of Dawson's integral may be obtained by the above formula and term-by-term integration:

$$\int_0^x D(\xi)\,d\xi = [1 - \exp(-x^2)]/4\pi^{1/2}$$

$$+ \sum_{n=1}^{\infty} [\mathrm{erf}(x - \tfrac{1}{2}n) - \mathrm{erf}(x + \tfrac{1}{2}n) + 2\,\mathrm{erf}(\tfrac{1}{2}n)]/4n\,.$$

The upper limit of the sum may be 50 with entirely adequate precision. The error function may be computed using

$$\mathrm{erf}{-}x = \mathrm{erf}\,|x|$$

and

$$\mathrm{erf}\,x \cong 1 - \frac{1}{(1 + x(a_1 + x(a_2 + x(a_3 + x(a_4 + xa_5)))))^8}$$

for $x \geq 0$, where

$$a_1 = 0.141\,128\,2\,, \qquad a_2 = 0.088\,640\,3\,, \qquad a_3 = 0.027\,433\,5\,,$$

$$a_4 = -0.000\,394\,5\,, \qquad a_5 = 0.003\,289\,8\,.$$

TABLE III. Bibliography. Reference entries are grouped according to their relation to various aspects of laser-beam self-focusing and track formation.

Topic	Refs.
Laser damage in transparent solid dielectrics: articles specifically describing track formation	1–20
Laser damage in transparent solid dielectrics: articles describing other types of laser damage	21–57
Laser-beam trapping in liquids	58–98
Steady-state beam trapping	99–130
Roles of Kerr effect vs electrostriction in beam trapping	131–140
Miscellaneous	141–153

[1] R. R. Alfano *et al.*, Phys. Rev. Letters **24**, 592 (1970). (See Table III above for organization of references.)

[2] T. P. Belikova and E. A. Sviridenkov, Zh. Eksperim. i Teor. Fiz. Pis'ma v Redaktsiyu **1**, 171 (1965) [Sov. Phys. JETP Letters **1**, 171 (1965)].

[3] J. P. Budin *et al.*, Appl. Phys. Letters **9**, 291 (1966).

[4] J-C. Buges *et al.*, Compt. Rend. **264B**, 871 (1967).

[5] W. Engelhardt, Appl. Phys. Letters **15**, 216 (1969).

[6] I. L. Fabelinskii *et al.*, Appl. Opt. **6**, 1793 (1967).

[7] M. Hercher, J. Opt. Soc. Am. **54**, 563 (1964).

[8] L. D. Khazov *et al.*, Opt. i Spektroskopiya **25**, 453 (1968) [Opt. Spectry. (USSR) **25**, 248 (1968)].

[9] N. I. Lipatov *et al.*, Zh. Eksperim. i Teor. Fiz.

Pis'ma v Redaktsiyu **11**, 444 (1970) [Sov. Phys. JETP Letters **11**, 300 (1970)].

[10] D. I. Mash *et al.*, Zh. Eksperim. i Teor. Fiz. Pis'ma v Redaktsiyu **2**, 246 (1965) [Sov. Phys. JETP Letters **2**, 157 (1965)].

[11] A. V. Shatilov *et al.*, Sov. J. Opt. Tech. **36**, 329 (1969).

[12] G. N. Steinberg, Perkin-Elmer Corporation Report No. 7735, 1964 (unpublished). See preceding paper [Phys. Rev. A **4**, 1182 (1971)] for further details.

[13] G. N. Steinberg *et al.*, Perkin-Elmer Corporation Report No. 7803, 1964 (unpublished).

[14] G. N. Steinberg *et al.*, Perkin-Elmer Corporation Report No. 7883, 1964 (unpublished).

[15] G. M. Zverev *et al.*, Zh. Eksperim. i Teor. Fiz. **53**, 1848 (1970) [Sov. Phys. JETP **26**, 1053 (1968)].

[16] G. M. Zverev *et al.*, Zh. Eksperim. i Teor. Fiz. Pis'ma v Redaktsiyu **9**, 108 (1969) [Sov. Phys. JETP Letters **9**, 61 (1969)].

[17] G. M. Zverev *et al.*, Zh. Eksperim. i Teor. Fiz. Pis'ma v Redaktsiyu **5**, 391 (1967) [Sov. Phys. JETP Letters **5**, 319 (1967)].

[18] G. M. Zverev *et al.*, Zh. Eksperim. i Teor. Fiz. Pis'ma v Redaktsiyu **6**, 391 (1967) [Sov. Phys. JETP Letters **6**, 351 (1967)].

[19] G. M. Zverev *et al.*, Zh. Eksperim. i Teor. Fiz. **57**, 730 (1969) [Sov. Phys. JETP **30**, 400 (1970)].

[20] G. M. Zverev *et al.*, Zh. Eksperim. i Teor. Fiz. **57**, 1128 (1969) [Sov. Phys. JETP **30**, 616 (1970)].

[21] R. R. Alfano *et al.*, Phys. Rev. Letters **24**, 584 (1970).

[22] B. M. Ashkinadze *et al.*, Zh. Eksperim. i Teor. Fiz. **50**, 1187 (1966) [Sov. Phys. JETP **23**, 788 (1966)].

[23] B. M. Ashkinadze *et al.*, Dokl. Acad. Nauk SSSR **169**, 1041 (1966) [Sov. Phys. Doklady **11**, 703 (1967)].

[24] P. V. Avizonis *et al.*, Appl. Phys. Letters **7**, 205 (1965).

[25] G. I. Barenblatt *et al.*, Zh. Eksperim. i Teor. Fiz. **54**, 1337 (1968) [Sov. Phys. JETP **27**, 716 (1968).

[26] G. I. Barenblatt *et al.*, Zh. Eksperim. i Teor. Fiz. Pis'ma v Redaktsiyu **5**, 85 (1967) [Sov. Phys. JETP Letters **5**, 69 (1967)].

[27]T. P. Belikova *et al.*, Zh. Eksperim. i Teor. Fiz. Pis'ma v Redaktsiyu 3, 394 (1966) [Sov. Phys. JETP Letters 3, 257 (1966)].

[28]T. P. Belikova *et al.*, Zh. Eksperim. i Teor. Fiz. 54, 37 (1968) [Sov. Phys. JETP 27, 19 (1968)].

[29]A. A. Borshch *et al.*, Zh. Eksperim. i Teor. Fiz. 58, 26 (1970) [Sov. Phys. JETP 31, 15 (1970)].

[30]D. J. Bradley *et al.*, Brit. J. Appl. Phys. 17, 1221 (1966).

[31]J. P. Budin *et al.*, Electronics Letters 3, 31 (1967).

[32]J. H. Cullom *et al.*, Appl. Opt. 3, 989 (1964).

[33]Yu. K. Danileiko *et al.*, Zh. Eksperim. i Teor. Fiz. 58, 31 (1970) [Sov. Phys. JETP 31, 18 (1970)].

[34]J. Davit *et al.*, Compt. Rend 261, 3567 (1965).

[35]J. Davit *et al.*, Rev. Phys. Appl. 3, 118 (1968).

[36]J. Davit, J. Appl. Phys. 39, 6052 (1968).

[37]H. Dupont *et al.*, Appl. Phys. Letters 11, 271 (1967).

[38]J. Duvernoy, Opt. Commun. 1, 202 (1969).

[39]A. J. Gibson, Brit. J. Appl. Phys. 1, 933 (1968).

[40]C. R. Giuliano, Appl. Phys. Letters 5, 137 (1964).

[41]E. Harnik *et al.*, J. Opt. Soc. Am. 59, 840 (1969).

[42]D. W. Harper, Brit. J. Appl. Phys. 16, 751 (1965).

[43]H. Kusakawa *et al.*, J. Appl. Phys. 40, 3954 (1969).

[44]J. Martinelli, J. Appl. Phys. 37, 1939 (1966).

[45]R. A. Miller *et al.*, Appl. Opt. 6, 164 (1967).

[46]G. Nath *et al.*, Z. Naturforsch. 23A, 624 (1968).

[47]D. Olness, J. Appl. Phys. 39, 6 (1968).

[48]D. Olness, Appl. Phys. Letters 8, 283 (1966).

[49]V. A. Pashkov *et al.*, Zh. Eksperim. i Teor. Fiz. 51, 777 (1966) [Sov. Phys. JETP 24, 516 (1967)].

[50]B. F. Ponomarenko *et al.*, Zh. Eksperim. i Teor. Fiz. 54, 776 (1968) [Sov. Phys. JETP 27, 415 (1968)].

[51]A. I. Ritus *et al.*, Zh. Eksperim. i Teor. Fiz. Pis'ma v Redaktsiyu 6, 927 (1967) [Sov. Phys. JETP Letters 6, 349 (1967)].

[52]C. H. Skeen, *et al.*, Appl. Opt. 5, 1463 (1966).

[53]E. A. Sviridenkov, Fiz. Tverd. Tela. 9, 2442 (1967) [Sov. Phys. Solid State 9, 1917 (1968)].

[54]N. V. Volkova *et al.*, Fiz. Tverd. Tela 8, 2668 (1966) [Sov. Phys. Solid State 8, 2133 (1967)].

[55]N. V. Volkova *et al.*, Fiz. Tverd. Tela 8, 3595 (1966) [Sov. Phys. Solid State 8, 2872 (1968)].

[56]P. Whiteman *et al.*, Nature 208, 66 (1965).

[57]Y. Yasojima *et al.*, Japan J. Appl. Phys. 7, 552 (1968).

[58]N. Bloembergen *et al.*, Bull. Am. Phys. Soc. 10, 1129 (1965).

[59]N. Bloembergen *et al.*, IEEE J. Quant. Electron. QE-2, 246 (1966).

[60]R. G. Brewer, Phys. Rev. Letters 19, 8 (1967).

[61]R. G. Brewer *et al.*, Phys. Letters 23, 79 (1966).

[62]R. G. Brewer *et al.*, Phys. Rev. 166, 326 (1968).

[63]R. G. Brewer *et al.*, Phys. Rev. Letters 21, 267 (1968).

[64]R. G. Brewer *et al.*, Phys. Rev. Letters 18, 196 (1967).

[65]A. C. Cheung *et al.*, Phys. Rev. Letters 20, 786 (1968).

[66]R. Y. Chiao *et al.*, IEEE J. Quant. Electron QE-2, 467 (1966).

[67]R. Y. Chiao *et al.*, Bull. Am. Phys. Soc. 12, 686 (1967).

[68]Yu. S. Chilingarian, Zh. Eksperim. i Teor. Fiz. 55, 1589 (1969) [Sov. Phys. JETP 28, 832 (1969)].

[69]M. M. Denariez-Roberge *et al.*, Appl. Phys. Letters

[14], 205 (1969).

[70]M. J. Freiser *et al.*, Phys. Letters 24A, 683 (1967).

[71]E. Garmire *et al.*, Phys. Rev. Letters 16, 347 (1966).

[72]T. K. Gustafson *et al.*, Phys. Rev. 177, 306 (1969).

[73]T. K. Gustafson *et al.*, Appl. Phys. Letters 12, 165 (1968).

[74]G. Hauchecorne *et al.*, Compt. Rend. 261, 4014 (1965).

[75]H. A. Haus *et al.*, IEEE J. Quant. Electron. QE-4, 519 (1968).

[76]R. W. Hellwarth, Phys. Rev. 152, 156 (1966).

[77]R. J. Joenk *et al.*, Phys. Letters 24A, 228 (1967).

[78]W. Kaiser *et al.*, Phys. Letters 22, 60 (1966).

[79]J. B. Keller, Courant Institute for Mathematical Sciences report, 1968 (unpublished).

[80]S. Kielich, Phys. Letters 25A, 153 (1967).

[81]V. V. Korobkin *et al.*, Zh. Eksperim. i Teor. Fiz. Pis'ma v Redaktsiyu 11, 153 (1970) [Sov. Phys. JETP Letters 11, 94 (1970)].

[82]P. Lallemand *et al.*, Phys. Rev. Letters 15, 1010 (1965).

[83]J. R. Lifsitz *et al.*, Appl. Phys. Letters 13, 245 (1968).

[84]M. T. Loy *et al.*, Appl. Phys. Letters 14, 380 (1969).

[85]M. T. Loy, Phys. Rev. Letters 22, 994 (1969).

[86]M. Maier *et al.*, Phys. Rev. Letters 24, 352 (1970).

[87]P. D. Maker *et al.*, Phys. Rev. Letters 12, 507 (1964).

[88]G. Mayer *et al.*, Compt. Rend. 258, 2039 (1964).

[89]P. D. McWane *et al.*, Appl. Phys. Letters 8, 278 (1966).

[90]R. Polloni *et al.*, Phys. Rev. Letters 23, 690 (1969).

[91]N. F. Pilipentskii *et al.*, Zh. Eksperim. i Teor. Fiz. Pis'ma v Redaktsiyu 2, 88 (1965) [Sov. Phys. JETP Letters 2, 55 (1965)].

[92]C. L. Riddiford *et al.*, J. Physics D 3, 1314 (1970).

[93]S. Saikan *et al.*, IEEE J. Quant. Electron. QE-4, 618 (1968).

[94]J. Sarfatt, Phys. Letters 26A, 88 (1967).

[95]Y. R. Shen *et al.*, Phys. Rev. Letters 19, 1171 (1967).

[96]A. P. Veduta, Zh. Eksperim. i Teor. Fiz. Pis'ma v Redaktsiyu 5, 154 (1967) [Sov. Phys. JETP Letters 5, 124 (1967)].

[97]C. C. Wang, Phys. Rev. Letters 16, 344 (1966).

[98]C. C. Wang, Phys. Rev. 152, 149 (1966).

[99]D. I. Abakarov *et al.*, Zh. Eksperim. i Teor. Fiz. 52, 463 (1967) [Sov. Phys. JETP 25, 303 (1967).

[100]A. A. Abramov *et al.*, Zh. Eksperim. i Teor. Fiz. Pis'ma v Redaktsiyu 9, 675 (1969) [Sov. Phys. JETP Letters 9, 419 (1969)].

[101]S. A. Akhmanov *et al.*, Zh. Eksperim. i Teor. Fiz. 50, 1537 (1966) [Sov. Phys. JETP 23, 1025 (1966)].

[102]S. A. Akhmanov *et al.*, Zh. Eksperim. i Teor. Fiz. 51, 296 (1966) [Sov. Phys. JETP 24, 198 (1967)].

[103]S. A. Akhmanov *et al.*, Usp. Fiz. Nauk 93, 19 (1967) [Sov. Phys. Usp. 10, 609 (1968)].

[104]G. A. Askar'yan, Zh. Eksperim. i Teor. Fiz. 42, 1567 (1962) [Sov. Phys. JETP 15, 1088 (1962)].

[105]G. A. Askar'yan *et al.*, Zh. Eksperim. i Teor. Fiz. Pis'ma v Redaktsiyu 10, 113 (1969) [Sov. Phys. JETP Letters 10, 71 (1969)].

[106]V. I. Bespalov *et al.*, Zh. Eksperim. i Teor. Fiz. Pis'ma v Redaktsiyu 3, 471 (1966) [Sov. Phys. JETP

Letters 3, 307 (1966)].

[107]R. Y. Chiao et al., Phys. Rev. Letters 13, 479 (1964).

[108]A. L. Dyshko et al., Zh. Eksperim. i Teor. Fiz. Pis'ma v Redaktsiyu 6, 665 (1967) [Sov. Phys. JETP Letters 6, 146 (1967)].

[109]A. L. Dyshko, et al., Dokl. Akad. Nauk SSSR 188, 792 (1969) [Sov. Phys. Doklady 14, 976 (1970)].

[110]V. M. Eleonskii et al., Zh. Eksperim. i Teor. Fiz. 56, 574 (1969) [Sov. Phys. JETP 29, 317 (1969)].

[111]V. M. Eleonskii et al., Zh. Eksperim. i Teor. Fiz. 57, 478 (1969) [Sov. Phys. JETP 30, 262 (1970)].

[112]J. A. Fleck, Jr., et al., Appl. Phys. Letters 15, 313 (1969).

[113]H. A. Haus, Appl. Phys. Letters 8, 128 (1966).

[114]P. L. Kelly, Phys. Rev. Letters 15, 1005 (1965).

[115]V. N. Lugovoi, Dokl. Akad. Nauk SSSR 176, 58 (1967) [Sov. Phys. Doklady 12, 866 (1968)].

[116]V. N. Lugovoi et al., Zh. Eksperim. i Teor. Fiz. Pis'ma v Redaktsiyu 7, 153 (1968) [Sov. Phys. JETP Letters 7, 117 (1968)].

[117]P. D. McWane, Nature 211, 1081 (1966).

[118]A. H. Piekara, Appl. Phys. Letters 13, 225 (1968).

[119]Yu. P. Raizer, Zh. Eksperim. i Teor. Fiz. Pis'ma v Redaktsiyu 4, 3 (1966) [Sov. Phys. JETP Letters 4, 1 (1966)].

[120]J. D. Reichert et al., IEEE J. Quant. Electron. QE-4, 221 (1968).

[121]P. A. Silberg, Phys. Rev. 153, 342 (1967).

[122]V. I. Talanov, Izv. v Radiofiz. 9, 410 (1966) [Sov. Radiophys. 9, 260 (1966)].

[123]V. I. Talanov, Zh. Eksperim. i Teor. Fiz. Pis'ma v Redaktsiyu 2, 218 (1965) [Sov. Phys. JETP Letters 2, 138 (1965)].

[124]V. I. Talanov, Zh. Eksperim. i Teor. Fiz. Pis'ma v Redaktsiyu 11, 303 (1970) [Sov. Phys. JETP Letters 11, 199 (1970)].

[125]J. P. Taran et al., IEEE J. Quant. Electron. QE-5, 381 (1969).

[126]S. N. Vlasov et al., Appl. Opt. 9, 1486 (1970).

[127]C. Wang, Phys. Rev. 173, 908 (1968).

[128]J. W. F. Woo, Appl. Phys. Letters 15, 200 (1969).

[129]Z. K. Yankauskas, Izv. v Radiofiz. 9, 412 (1966) [Sov. Radiophys. 9, 261 (1966)].

[130]V. E. Zakharov, Zh. Eksperim. i Teor. Fiz. 53, 1735 (1968) [Sov. Phys. JETP 26, 994 (1968)].

[131]K. A. Brueckner et al., Phys. Rev. Letters 17, 78 (1966).

[132]K. A. Brueckner et al., Phys. Rev. 164, 182 (1967).

[133]K. A. Brueckner et al., Phys. Rev. 175, 332 (1968).

[134]A. A. Chaban, Zh. Eksperim. i Teor. Fiz. Pis'ma v Redaktsiyu 6, 487 (1967) [Sov. Phys. JETP Letters 6, 20 (1967)].

[135]D. H. Close et al., IEEE J. Quant. Electron. QE-2, 553 (1966).

[136]Yu. P. Raizer, Zh. Eksperim. i Teor. Fiz. Pis'ma v Redaktsiyu 4, 286 (1966) [Sov. Phys. JETP Letters 4, 193 (1966)].

[137]Yu. P. Raizer, Zh. Eksperim. i Teor. Fiz. 52, 470 (1967) [Sov. Phys. JETP 25, 308 (1967)].

[138]Y. R. Shen et al., Phys. Rev. 163, 224 (1967).

[139]Y. R. Shen, Phys. Letters 20, 378 (1966).

[140]Ya. B. Zel'dovich et al., Zh. Eksperim. i Teor. Fiz. Pis'ma v Redaktsiyu 3, 137 (1966) [Sov. Phys. JETP Letters 3, 86 (1966)].

[141]E. L. Kerr, in Damage in Laser Glass (American Society For Testing and Materials, Philadelphia, 1969), p. 23.

[142]E. S. Bliss, in Damage in Laser Glass (American Society for Testing and Materials, Philadelphia, 1969), p. 9.

[143]P. K. Tien et al., Proc. IEEE 53, 129 (1965).

[144]H. N. Ritland, J. Am. Ceram. Soc., 38, 86 (1955).

[145]J. F. Nye, Physical Properties of Crystals (Clarendon, Oxford, England, 1957), p. 243.

[146]L. D. Landau and X. Lifshitz, Electrodynamics of Continuous Media (Addison-Wesley, New York, 1960), p. 69.

[147]J. R. Pierce, Theory and Design of Electron Beams (Van Nostrand, Princeton, N. J., 1954), p. 195.

[148]J. R. Pierce, Proc. Natl. Acad. Sci. 47, 1808 (1961).

[149]W. G. Wagner et al., Phys. Rev. 175, 256 (1968).

[150]H. Goldstein, Classical Mechanics (Addison-Wesley, Reading, Mass., 1950), p. 61.

[151]H. Kogelnik et al., Proc. IEEE, 54, 1312 (1966).

[152]C. R. Giuliano (private communication).

[153]Handbook of Mathematical Functions, edited by N. Abramowitz and I. A. Stegun, Natl. Bur. Std. (U. S. GPO, Washington, D. C., 1964), p. 319.